Deflagrations of localised homogeneous and inhomogeneous hydrogen-air mixtures in enclosures

DEFLAGRATIONS OF LOCALISED HOMOGENEOUS AND INHOMOGENEOUS HYDROGEN-AIR MIXTURES IN ENCLOSURES

D. Makarov[1], P. Hooker[2], M. Kuznetsov[3], V. Molkov[1]
[1]Hydrogen Safety Engineering and Research Centre (HySAFER), Ulster University, Newtownabbey, BT37 0QB, UK
[2]Health and Safety Executive, Harpur Hill, Buxton, SK17 9JN, UK
[3]Karlsruhe Institute of Technology, 76344 Eggenstein-Leopoldshafen, Germany

Abstract
Two original models for use as novel tools for the design of hydrogen-air deflagration mitigation systems for equipment and enclosures are presented. The first model describes deflagrations of localised hydrogen-air mixtures in a closed space such as a pressure vessel or a well-sealed building while the second model defines safety requirements for vented deflagrations of localised mixtures in an enclosure. Examples of localised mixtures include 'pockets' of gas within an enclosure as well as stratified gas distributions which are especially relevant to hydrogen releases. The thermodynamic model for closed spaces is validated against experiments available from the literature. This model is used to estimate the maximum hydrogen inventory in a closed space assuming the closed space can withstand a maximum overpressure of 10 kPa without damage (this is typical of many civil structures). The upper limit for hydrogen inventory in a confined space to prevent damage is found to be equivalent to 7.9% of the closed space being filled with 4% hydrogen. If the hydrogen inventory in a closed space is above this upper limit then the explosion has to be mitigated by the venting technique. For the first time an engineering correlation is presented that accounts for the phenomena affecting the overpressure from localised vented deflagrations, i.e. the turbulence generated by the flame front itself, the preferential diffusion in stretched flames, the fractal behaviour of the turbulent flame front surface, the initial flow turbulence in unburnt mixture, and the increase of the flame surface area due to the shape of an enclosure. Validation of the new vented deflagration model developed at Ulster has been carried out against 25 experiments with lean stratified hydrogen-air mixtures performed by the Health and Safety Executive (UK) and Karlsruhe Institute of Technology (Germany).

Keywords: Hydrogen, localised flammable mixture, vented deflagration, inhomogeneous mixture, engineering correlation, validation.

Nomenclature

A	fraction of vent area occupied by combustion products, or coefficient in equation (49)
B	coefficient in equation (49)
Br_t	turbulent Bradley number, $Br_t = \left(\sqrt{E_i/\gamma}\,\mu F c_{ui}\right)\left((36\pi_0)^{1/3}\,\Xi V^{2/3} S_{u_i}\,(E_i-1)\right)$
Br_t^*	parameter for scaling overpressure in equation (60)
c_p	specific heat at constant pressure in equations (8) and (12) (J/kg/K)
c_v	specific heat at constant volume in equation (20) (J/mol/K)
c_{ui}	speed of sound in unburnt mixture (m/s), $c_{ui} = \sqrt{\gamma RT/M}$
D	fractal dimension
e	energy per unit mass (J/kg)
E_i	combustion products expansion coefficient, $E_i = M_{ui}T_{bi}/M_{bi}T_{ui}$
F	vent area (m^2)
G	mass flow rate (kg/s)
H	height (m), or enthalpy (J)
ΔH_c	heat of combustion (J/mol)
Δh_c	heat of combustion (J/kg)
h	enthalpy per unit mass (J/kg)
L	length (m)
M	molecular mass (g/mol)

m mass (kg), or burning velocity temperature index (Table7)
n mass fraction, or burning velocity baric index (Table7)
p pressure (Pa abs)
q heat per unit mass (J/kg)
R flame radius (m), or universal gas constant, R=8314 (J/K/kmol)
$R^{\#}$ non-dimensional venting parameter, $R^{\#} = \left\{(2\gamma)/(\gamma-1)\pi\sigma\left[(1/\pi)^{2/\gamma} - (1/\pi)^{1+1/\gamma}\right]\right\}^{1/2}$
R_0 critical radius for transition from laminar to fully turbulent flame propagation regime (m)
S_t turbulent burning velocity (m/s)
S_u laminar burning velocity (m/s)
T temperature (K)
t time (s)
u internal energy per unit mass (J/kg)
V volume (m^3)
v specific volume (m^3/kg)
W width (m), or non-dimensional venting parameter, $W = \mu F c_{ui} / \left[(36\pi_0)^{1/3}\sqrt{\gamma_u} V^{2/3} S_{ui}\right]$
w mechanical work of gas per unit mass (J/kg)
x_{H2} volumetric fraction of hydrogen in entire enclosure, $x_{H2} = \varphi \cdot \Phi$
Z non-dimensional number, $Z = \gamma_b\left[E_i - (\gamma_u/\gamma_b)(\gamma_b-1)/(\gamma_u-1)\right]\pi^{(1-\gamma_u)/\gamma_u} + (\gamma_u-\gamma_b)/(\gamma_u-1)$

Greek

Φ volumetric fraction of localised flammable fuel-air mixture in enclosure
Φ^* volumetric fraction of the fastest burning fuel-air mixture in enclosure
γ adiabatic index, $\gamma=c_p/c_v$
φ volumetric fraction of fuel in localised fuel-air mixture, and number of moles in equations (9)-(11)
μ discharge coefficient
π non-dimensional pressure $\pi = p/p_i$
π_0 "Pi" number, 3.14159
Ξ/μ deflagration-outflow interaction (DOI) number, $\Xi/\mu = \Xi_K \Xi_{LP} \Xi_{FR} \Xi_{u'} \Xi_{AR} \Xi_O$
Ψ empirical coefficient
Ξ_K wrinkling factor to account for the turbulence generated by the flame front itself
Ξ_{LP} wrinkling factor to account for the leading point flame acceleration mechanism
Ξ_{FR} wrinkling factor to account for the fractal increase of the flame surface area
$\Xi_{u'}$ wrinkling factor to account for the initial flow turbulence in unburnt mixture
Ξ_{AR} wrinkling factor to account for the aspect ratio of the enclosure
Ξ_O wrinkling factor to account for the presence of obstacles
ρ density (kg/m^3), $\rho = pM/(RT)$
σ relative density, $\sigma = \rho/\rho_i$
τ non-dimensional time, $\tau = t S_{u_i}/c_{u_i}$
ω volume fraction in enclosure

Subscripts

air air
b burnt mixture
corr correlation value
exp experimental value
f fuel
H2 hydrogen
i initial conditions
MAX maximum
MIN minimum
m flammable mixture
t turbulent
u unburnt mixture
0 initial thermodynamic state (before combustion)
1 thermodynamic state 1 (on completion of adiabatic isochoric combustion)
2 thermodynamic state 2 (on completion of adiabatic expansion)

Superscripts

‘ value in flammable mixture

Acronyms

BOS Background Oriented Schlieren
CFD Computational Fluid Dynamics
DOI Deflagration-Outflow Interaction
LES Large Eddy Simulation
RHS Right-Hand Side
SGS Sub-Grid Scale

1 Introduction

Deflagration of inhomogeneous, e.g. stratified, fuel-air mixtures in an enclosure, where fuel concentration varies mainly in vertical direction, is a realistic accident scenario for both industrial environment and domestic premises [1, 2]. This scenario may result from a slow release of heavier or lighter than air flammable gas, or a spill of flammable liquid, leading to formation of flammable layer near the floor or ceiling. The combustion of hydrogen-air-steam mixtures is of interest in the analysis of postulated post-accident nuclear containment events [3]. Mitigation of hydrogen-air deflagrations in realistic scenarios with inhomogeneous layers is on the research agenda due to the ongoing deployment of hydrogen systems and infrastructure in different countries around the globe.

Flammable stratified fuel-air mixture could occupy either the whole volume of an enclosure or only a part of the volume. Currently, the design of gaseous and dust explosion mitigation system by venting technique for partial-volume deflagrations presumes that the entire enclosure volume is occupied by the flammable mixture [1,4]. On the other hand, it is an established fact that deflagrations in mixtures with concentration gradient may be more dangerous than those in uniform mixtures with the same amount of released flammable gas [3].

Stamps et al. reviewed publications on combustion of localised mixtures in closed vessels [5]. Theoretical work on dynamics of partial combustion in a closed vessel was traced back to work by Flamm and Mache [6], and Lewis and von Elber [7]. Most of the work in those studies was aimed at finding the burning velocity from measured pressure-time history in closed vessels. Another group of models was focused on maximum deflagration pressure in closed vessel using thermodynamic equilibrium approach. For example, Sibulkin [8] considered localised mixture combustion as expansion process with heat transfer and work interaction. He applied the first law of thermodynamics assuming that pressure in the work term was constant and equal to the initial one, which restricted the model to relatively low overpressures. Babkin et al. [9] considered a closed system of unburnt, burnt and inert mixture. They used the conservation of volume and internal energy, as well as the equality of enthalpy across the flame front to obtain expression connecting maximum overpressure, mass fraction of unburnt mixture, and expansion coefficient. Boyack et al. [10] studied localised mixture combustion based on thermodynamic principles. They separated the process into two stages: complete combustion in a constant volume, and expansion of combustion products. Their model was based on the conservation of entire system energy, mass and the assumption of isentropic expansion of combustion products and compression of inert gas.

The first lumped parameter models of vented deflagration dynamics were developed and published by Yao [11] and Pasman et al. [12]. Later more detailed vented deflagration theories were developed by Bradley and Mitcheson in 1978 [13], and by Molkov and Nekrasov in 1984 [14]. All these studies considered vented deflagrations for cases when the entire enclosure is occupied by homogeneous flammable mixture. More publications on vented deflagrations for fully occupied by flammable mixture enclosure could be mentioned, including work at FM Global, e.g. [1,15,16], and at Ulster, e.g. [4,17-19].

All mentioned above models are based on assumption that flame propagation is significantly lower than the speed of sound and pressure rise is uniform across enclosure. Thus lumped parameter models are

anable to predict high overpressures in a particular enclosure location due to, e.g. local flame acceleration through a congested region, as it was experimentally observed in flat hydrogen-air layers by Friedrich et al. [20]. Successful use of a more sophisticated CFD method for resolution of such local effects was demonstrated in [21], where simulation of the stratified layer deflagration experiments [20] were performed.

In 2001 a comparative study of a number of vent sizing correlations for enclosures fully occupied by flammable mixture was carried out by Razus and Krause [22]. The more recent comparison of different modelling approaches for simulation of uniform hydrogen-air mixture vented deflagrations may be found in [23, 24, 25] and for various fuel-air compositions – in [26]. To the best of authors' knowledge the correlations for vent sizing, including NFPA 68 standard "Guide for venting of deflagrations" [27], do not include correlations validated for localised homogeneous and inhomogeneous mixture deflagrations.

The paper aims to develop and validate novel engineering models for localised deflagrations in closed and vented enclosures. The thermodynamic model for localised uniform mixture deflagration overpressure in a closed building is validated against experimental data [5]. Validation of the model for localised uniform and non-uniform vented deflagration is carried out against unique experiments with hydrogen-air mixtures in two enclosures: 1 m^3 volume chamber at Karlsruhe Institute of Technology (KIT, Germany) [28], and in 31 m^3 volume container at Health and Safety Executive (HSE, UK) [24]. The study will underpin the design of inherently safer hydrogen systems and infrastructure.

2 Thermodynamic model of localised mixture deflagration in a closed space

2.1 Model formulation

The model for calculation of maximum overpressure of localised uniform mixture deflagration in a closed space is based on thermodynamics principles and the assumption of thermodynamic equilibrium after combustion. Pressure dynamics is out of the scope in this model. Let us consider an enclosure with initial temperature of gases T_0 and pressure p_0. Figure 1 shows the enclosure, which is partially filled with homogeneous flammable fuel-air mixture occupying volume fraction of the enclosure Φ, and the rest of the enclosure is filled with non-reacting "inert" gas, e.g. air, of volume fraction $(1 - \Phi)$. The mass of fuel in the flammable mixture is m_f, the total mass of flammable mixture is m_m, its molar mass is M_m, and its volume is V_{m0}. The mass of non-reacting gas (air) is m_{air}, and the volume of air at initial state is V_{air0}.

Final thermodynamic state parameters, i.e. pressure, temperature, and volume, depend on the final state of the system only. Following thermodynamics and similar to previous studies, e.g. Boyack et al. [10], we "split" combustion into two stages: constant volume combustion of the initial fuel-air mixture within volume fraction of the enclosure Φ, and adiabatic expansion of the burnt fuel-air mixture inside the closed space. A schematic representation of these processes with parameters at initial state (state "0"), complete adiabatic isochoric combustion (state "1"), and adiabatic expansion of combustion products within the enclosure (state "2") is shown in Figure 1.

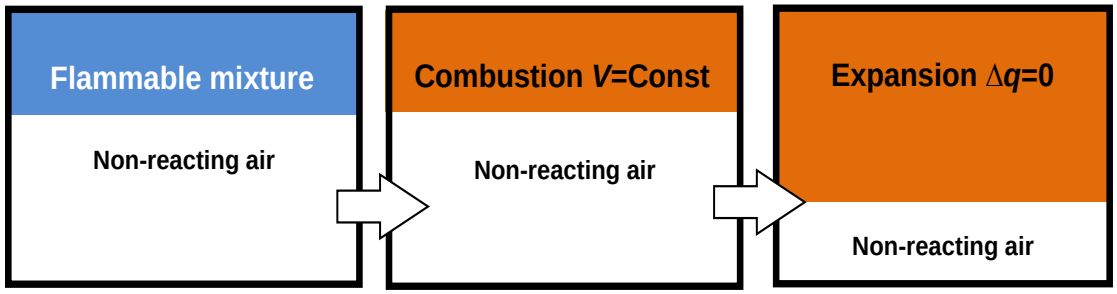

State "0": Initial state	State "1": Combustion V=Const	State "2": Expansion Δq=0
Initial state: T_0, p_0 Fuel-air mixture: m_m, M_m, V_{m0} Air: m_{air}, M_{air}, V_{air0}	Burnt mixture: m_b, T_{b1}, p_{b1} Air: m_{air}, M_{air}, T_0, ps_0	Final state of burnt mixture: T_{b2}, p_2, m_b, M_b, V_{b2} Final state of air: m_{air}, M_{air}, T_{air2}, p_2

Figure 1. Schematic problem formulation for localised deflagration in a closed space.

The analysis is based on the conservation of volume occupied at state "0" by unburnt localised flammable mixture and non-flammable gas (air) before combustion, and at state "2" by burnt mixture and the same amount of air, which are compressed at stage "2":

$$V_{m0} + V_{air0} = V_{b2} + V_{air2}\,. \tag{1}$$

This can be re-written using the perfect gas law as:

$$\frac{m_m}{M_m}\frac{RT_0}{p_0} + \frac{m_{air}}{M_{air}}\frac{RT_0}{p_0} = \frac{m_b}{M_b}\frac{RT_{b2}}{p_2} + \frac{m_{air}}{M_{air}}\frac{RT_{air2}}{p_2}, \tag{2}$$

and rearranged to:

$$\left(\frac{m_m}{M_m} + \frac{m_{air}}{M_{air}}\right)\frac{T_0}{p_0} = \frac{1}{p_2}\left(\frac{m_b}{M_b}T_{b2} + \frac{m_{air}}{M_{air}}T_{air2}\right). \tag{3}$$

The transition from state "1" to state "2" is the burnt mixture adiabatic expansion from pressure p_{b1} to p_2, and simultaneous adiabatic air compression from pressure p_0 to p_2. Then, equation (3) becomes:

$$\left(\frac{m_m}{M_m} + \frac{m_{air}}{M_{air}}\right)\frac{T_0}{p_0} = \frac{1}{p_2}\left(\frac{m_b}{M_b}T_{b1}\left(\frac{p_2}{p_{b1}}\right)^{\frac{\gamma_b-1}{\gamma_b}} + \frac{m_{air}}{M_{air}}T_0\left(\frac{p_2}{p_0}\right)^{\frac{\gamma_{air}-1}{\gamma_{air}}}\right), \tag{4}$$

from where we derive the equation for final deflagration pressure:

$$p_2 = \frac{p_0}{T_0}\frac{\frac{m_b}{M_b}T_{b1}\left(\frac{p_2}{p_{b1}}\right)^{\frac{\gamma_b-1}{\gamma_b}} + \frac{m_{air}}{M_{air}}T_0\left(\frac{p_2}{p_0}\right)^{\frac{\gamma_{air}-1}{\gamma_{air}}}}{\frac{m_m}{M_m}+\frac{m_{air}}{M_{air}}}. \quad (5)$$

Perfect gas law for the flammable mixture at state "0", for the burnt mixture at state "1", and the conservation of volume of flammable and burnt mixtures in the process "0-1" are, respectively:

$$\frac{m_m}{M_m} = \frac{p_0 V_m}{RT_0}; \quad \frac{m_b}{M_b} = \frac{p_{b1}V_{b1}}{RT_{b1}}; \; V_m = V_{b1}.$$

The ratio m_b/M_b can be then written in the form:

$$\frac{m_b}{M_b} = \frac{p_{b1}V_{b1}}{RT_{b1}}\frac{m_m}{M_m}\frac{RT_0}{p_0V_m} = \frac{m_m}{M_m}\frac{p_{b1}T_0}{p_0T_{b1}}.$$

Substitution of this result into (5) gives:

$$p_2 = \frac{p_0}{T_0}\frac{\frac{m_m}{M_m}\frac{p_{b1}T_0}{p_0T_{b1}}T_{b1}\left(\frac{p_2}{p_{b1}}\right)^{\frac{\gamma_b-1}{\gamma_b}} + \frac{m_{air}}{M_{air}}T_0\left(\frac{p_2}{p_0}\right)^{\frac{\gamma_{air}-1}{\gamma_{air}}}}{\frac{m_m}{M_m}+\frac{m_{air}}{M_{air}}} = \frac{\frac{m_m}{M_m}p_{b1}\left(\frac{p_2}{p_{b1}}\right)^{\frac{\gamma_b-1}{\gamma_b}} + \frac{m_{air}}{M_{air}}p_0\left(\frac{p_2}{p_0}\right)^{\frac{\gamma_{air}-1}{\gamma_{air}}}}{\frac{m_m}{M_m}+\frac{m_{air}}{M_{air}}}. \quad (6)$$

This equation may be simplified using the equality of molar and volumetric fractions and then using the conversion of mass to volume fractions:

$$\frac{m_m/M_m}{m_m/M_m + m_{air}/M_{air}} = \frac{\left(m_m/\left(m_m+m_{air}\right)\right)/M_m}{\left(m_m/\left(m_m+m_{air}\right)\right)/M_m + \left(m_{air}/\left(m_m+m_{air}\right)\right)/M_{air}} = \frac{\left(n_m\right)/M_m}{\left(n_m\right)/M_u + \left(n_{air}\right)/M_{air}} = \Phi;$$

$$\frac{m_{air}/M_{air}}{m_m/M_u + m_{air}/M_{air}} = \frac{\left(m_m/\left(m_m+m_{air}\right)\right)/M_a}{\left(m_m/\left(m_m+m_{air}\right)\right)/M_m + \left(m_{air}/\left(m_m+m_{air}\right)\right)/M_{air}} = \frac{\left(n_{air}\right)/M_{air}}{\left(n_m\right)/M_m + \left(n_{air}\right)/M_{air}} = 1-\Phi.$$

Substitution of above equations for volume fractions into equation (6) gives a sought transcendential equation for p_2, which may be solved iteratively, and where p_{b1} is yet to be defined:

$$p_2 = \Phi\, p_{b1}\left(\frac{p_2}{p_{b1}}\right)^{\frac{\gamma_b-1}{\gamma_b}} + \left(1-\Phi\right)p_0\left(\frac{p_2}{p_0}\right)^{\frac{\gamma_{air}-1}{\gamma_{air}}}. \quad (7)$$

This equation for p_2 is different from Boyack et al. [10] as a result of our approach. Pressure p_{b1} at state "1" (adiabatic isochoric combustion) may be obtained by using various methods. Here we describe two possible methods.

Method 1 to calculate p_{b1}

A procedure for calculation of burnt mixture pressure p_{b1} may be derived from the internal energy conservation equation for isohoric process, $u_{m0} = u_{b1}$. The process of adiabatic combustion with no heat input or loss, $\Delta q = 0$, at constant volume, i.e. no work done by gas, $\Delta w = 0$, does not involve any change of internal energy, i.e. $\Delta u = 0$. Internal energy u can be expressed via enthalpy h as $h_{b1} - p_{b1}v_0 = h_{m0} - p_0 v_0$. Using the perfect gas law $pv = RT/M$, the equation for enthalpy $h = h^0 + c_p\Delta T$, the mass conservation law $m_b = m_0$, and the assumption that initial temperature is equal to the temperature at which enthalpy of formation was specified, results in the following equation:

$$\left(h_b^0 - h_m^0\right) + T_{b1}\left(c_{p_b} - \frac{R}{M_b}\right) - T_0\left(c_{p_b} - \frac{R}{M_m}\right) = 0\,. \tag{8}$$

The first term on LHS is heat of combustion for the considered localised fuel-air mixture $\Delta h_c = h_b^0 - h_m^0$ (for exothermic reaction $\Delta h_c < 0$). Its simple algebraic expression may be written assuming a single-step reaction (here is given example for hydrogen):

$$\varphi H_2 + (1-\varphi)[0.21O_2 + 0.79N_2] = \varphi H_2O + (0.21 - 0.71\varphi)O_2 + (1-\varphi)0.79N_2\,. \tag{9}$$

Treating coefficient φ in (9) as number of moles, the mass of bunt mixture is:

$$m_b = \varphi(mol)\cdot 18\,(g/mol) + (0.21 - 0.71\varphi)(mol)\cdot 32\,(g/mol) + ((1-\varphi)0.79)(mol)\cdot 28\,(g/mol)\,. \tag{10}$$

As the masses of burnt and unburnt mixtures are the same, and the amount of unburnt mixture is 1 mole, the heat of reaction per 1 kg of flammable (or burnt) mixture may be calculated in either way:

$$\Delta h_c = \varphi\cdot\Delta H_c / m_m = \Delta H_c / M_m\,,$$

$$\Delta h_c = \varphi\cdot\Delta H_c / m_b =$$

$$= \frac{\varphi(mol)\cdot\Delta H_c\,[J/mol]}{\left(\varphi(mol)\cdot 18\left[\frac{g}{mol}\right] + (0.21 - 0.71\varphi)(mol)\cdot 32\left[\frac{g}{mol}\right] + (1-\varphi)0.79(mol)\cdot 28\left[\frac{g}{mol}\right]\right)\cdot 10^{-3}\left[\frac{kg}{g}\right]}\,. \tag{11}$$

Rearranging (8) for T_{b1} gives:

$$T_{b1} = \frac{T_0\left(c_{p_b} - R/M_m\right) - \Delta h_c}{c_{p_b} - R/M_b}\,. \tag{12}$$

Thus, the pressure corresponding to this closed volume combustion based on the perfect gas law, is:

$$p_{b1} = \frac{p_0 V_m M_m}{RT_0}\frac{RT_{b1}}{V_{b1}M_b} = p_0\frac{M_m T_{b1}}{M_b T_0}\,. \tag{13}$$

For calculations of hydrogen-air mixture deflagration overpressure p_2 (see below) the hydrogen heat of combustion was adopted as $\Delta h_c = -2.44\cdot 10^5$ J/mol. Specific heats of water vapour H_2O, oxygen O_2 and nitrogen N_2 were calculated using respectively the following polinomilas [29]:

$$c_{p_{H2O}} = 1563.08 + 1.604\cdot T - 2.933\cdot 10^{-3}\cdot T^2 + 3.216\cdot 10^{-6}\cdot T^3 - 1.157\cdot 10^{-9}\cdot T^4 \quad (T\leq 1000\text{ K})$$
$$\text{and } = 1233.23 + 1.411\cdot T - 4.029\cdot 10^{-4}\cdot T^2 + 5.543\cdot 10^{-8}\cdot T^3 - 2.940\cdot 10^{-12}\cdot T^4 \quad (T>1000\text{ K}),$$

$$c_{p_{O2}} = 834.83 + 0.2930\cdot T - 1.496\cdot 10^{-4}\cdot T^2 + 3.414\cdot 10^{-7}\cdot T^3 - 2.278\cdot 10^{-10}\cdot T^4 \quad (T\leq 1000\text{ K})$$
$$\text{and } = 960.75 + 0.1594\cdot T - 3.271\cdot 10^{-5}\cdot T^2 + 4.613\cdot 10^{-9}\cdot T^3 - 2.953\cdot 10^{-13}\cdot T^4 \quad (T>1000\text{ K}),$$

$$c_{p_{N2}} = 979.04 + 0.4180\cdot T - 1.176\cdot 10^{-3}\cdot T^2 + 1.674\cdot 10^{-6}\cdot T^3 - 7.256\cdot 10^{-10}\cdot T^4 \quad (T\leq 1000\text{ K})$$
$$\text{and } = 868.62 + 0.4416\cdot T - 1.683\cdot 10^{-4}\cdot T^2 + 2.997\cdot 10^{-8}\cdot T^3 - 2.004\cdot 10^{-12}\cdot T^4 \quad (T>1000\text{ K}).$$

The system of equations (7), (11)-(13) forms the model, which may be now solved for the localised mixture maximum deflagration pressure p_2.

Method 2 to calculate p_{b1}

Calculation of adiabatic flame temperature (12) and closed vessel pressure (13) can be done using thermodynamic equilibrium model realised, for example, in GASEQ software [30] (constant volume adiabatic process with reactants N_2, O_2, H_2, H_2O, OH, H, O). For the lower flammability limit of

hydrogen $\varphi = 0.04$ the thermodynamic equilibrium solution by GASEQ provided higher adiabatic flame temperature T_{b1} by negligible 0.9% and a bit larger pressure p_{b1} by 3.3% than the solution of equations (12) and (13) (see Table 2 below).

2.2 The thermodynamic model validation

Stamps *et al*. [5] conducted experiments on combustion of localised hydrogen-air mixtures in the closed constant volume vessel. The vessel in the form of pipe was filled in partially by hydrogen-air mixture separated by a piston from an inert gas (carbon dioxide, helium, nitrogen). When hydrogen-air mixture deflagrated the piston compressed the inert gas until pressure equilibration on both sides of the piston. The varied parameters included volume fraction of combustible gas, pressure in the burnt gas p_{b1} varied depending on the hydrogen concentration in unburnt mixture, and the type of the inert gas.

Experimental measurements [5] included burnt mixture pressure p_{b1}, for which a companion set of constant volume combustion tests was conducted filling the entire vessel with hydrogen-air mixtures. Table 1a gives comparison of the model solution (7) against experimental data [5] for varying flammable volume fraction Φ with constant hydrogen-air equivalence ratio 0.997 using experimental data on p_{b1}. Table 1a shows also predictions by the model of Boyack et al. [10] as done in [5]. The Ulster model scatter in prediction of p_2 is closer to experimental data while predictions by [10] are shifted to higher overpressures.

Table 1b compares the experimental results [5] with the derived equation (7) and the solution by Boyack et al. [10]. However, in Table 1b both models use pressure p_{b1} calculated independently from experiment by equations (11)-(13), which is more preferable as an engineering tool for safety design. Solution to the model by Boyack *et al.* [10] for such conditions is not available in [5] and was developed in this study. The analytical solution for p_{b1} (Table 1b) is higher than the experimental value of p_{b1} (Table 1a) due to heat losses; as a result the value of p_2 is higher for both models too. Yet, the derived here model predicts experimental data more favourably than the solution by Boyack *et al.* [10]. The predictions are conservative for all inert gases and all mixture volume fractions Φ.

2.3 The upper hydrogen inherently safer inventory limit

The developed and validated model may now be used to find out the maximum possible hydrogen inventory in a closed space like a warehouse (in the limit of negligible leaks), which, if released and deflagrated, will not generate deflagration overpressure that the enclosure cannot withstand for any possible distribution of fuel in air within flammability limits. Any leaks present in a realistic enclosure will decrease overpressure which will keep the model predictions on conservative side. Here, the solution is presented for the explosion overpressure (p_2-p_0)=10 kPa, which is adopted as a typical threshold value for damage to civil structures. More accurate assessment of overpressure damage to buildings may be found, e.g. in work by Baker *et al.* [31] who found that minor structural damage of a building can be produced by a blast wave with overpressure in the range of 4.8-17.0 kPa and impulse above 130 Pa·s, as well as for any overpressure above 4.8 kPa if the impulse is in the range 130-300 Pa·s. Alternatively, Mannan [32] suggested the following overpressure thresholds: 4.8 kPa for minor damage, 6.9 kPa for partial demolition, and 34.5 kPa for almost total destruction.

The volumetric fraction of hydrogen in unburnt mixture is denoted as φ. Table 2 shows values of volumetric fraction of unburnt mixture in the enclosure, Φ, which were calculated assuming that the deflagration overpressure is equal to 10 kPa. The table also presents burnt mixture pressure p_{b1} and temperature T_{b1} at state "1" calculated using equations (11)-(13). The averaged throughout the entire enclosure volumetric fraction of hydrogen is then $x_{H2} = \varphi \cdot \Phi$. Let us derive the upper limit of hydrogen inventory, i.e. averaged through the entire enclosure volumetric fraction of stored and released hydrogen,

as an easy calculated parameter for use in safety engineering design of hydrogen systems and infrastructure. This limit allows to define the hydrogen inventory in a closed building, which will not destroy the structure even if the localised mixture formed by release of this inventory deflagrated.

Table 2 demonstrates that higher concentrations of hydrogen can be ignored as they don't give conservative (lower) value of x_{H2} (x_{H2} increases with hydrogen concentration). By this reason the range of studied hydrogen concentrations is 4-20% by volume only. The value of volumetric fraction $x_{H2} = \varphi \cdot \Phi$ is minimum at hydrogen concentration 4% by volume (lower flammability limit, LFL) and equals to 0.00314, i.e. averaged throughout enclosure volume hydrogen concentration is 0.314% by volume. This specifies the upper limit on hydrogen inventory expressed as the volume of hydrogen allowable to be releases in a closed structure:

$$V_{H2} < 0.00314 \cdot V , \quad (14)$$

where V is the free enclosure volume. This solution may be expressed in terms of the upper hydrogen inventory limit in terms of mass, which could be more convenient tool in some situations:

$$m_{H2} < 2.61 \cdot 10^{-4} V , \quad (15)$$

where m_{H2} is the maximum mass of hydrogen (in kilograms) allowable to be released into volume V (in m^3), e.g. into a warehouse, assuming normal initial temperature and pressure.

Method 1 and method 2 give a difference in the upper hydrogen inventory limit within acceptable for hydrogen safety engineering value of only 1.3%. Thus, the upper hydrogen inventory limit, expressed in form (14) for volume or in form (15) for mass, can be considered as independent on the method of calculation of p_{b1}.

Table 1a. Comparison of experimental data, the model solution for p_2, equation (7), and solution by Boyack *et al.* [5]; both solutions are based on experimental data p_{b1}, hydrogen-air mixture equivalence ratio for all experiments is 0.997.

Inert gas	H_2-air mixture volume fraction Φ	p_0, kPa	Experimental pressure p_{b1}, kPa	Adiabatic index for burnt mixture γ_b	Inert gas volume fraction (1-Φ)	Adiabatic index for inert gas, to be used as γ_{air} in (7)	Experimental p_2, kPa [5]	Solution (7), this study		Solution by Boyack *et al*. as developed in [5]	
								p_2, kPa	error, %	p_2, kPa	error, %
CO2	0.4686	105.5	599.7	1.372	0.5314	1.289	295.7	305.2	3.18	346.7	17.2472
CO2	0.8783	109.3	632.1	1.372	0.1217	1.289	491.9	555.1	12.85	571.8	16.2431
He	0.4686	105.4	598.9	1.372	0.5314	1.667	335.8	326.0	-2.93	365.9	8.96367
He	0.8783	105.8	612.2	1.372	0.1217	1.667	553.1	546.1	-1.26	560.5	1.33791
N2	0.4686	104.7	595.4	1.372	0.5314	1.4	316.5	309.5	-2.22	350.3	10.6793
N2	0.8783	109.8	635.3	1.372	0.1217	1.4	530.1	560.7	5.77	576.9	8.82852

Table 1b. Comparison of experimental data, the model solution for p_2, equation (7), and solution by Boyack *et al.* [5]; both solutions are based on analytical value p_{b1} (equations (11)-(13)), hydrogen-air mixture equivalence ratio for all experiments is 0.997.

Inert gas	H_2-air mixture volume fraction Φ	p_0, kPa	Pressure p_{b1}, (11)-(13), kPa	Adiabatic index for burnt mixture γ_b	Inert gas volume fraction (1-Φ)	Adiabatic index for inert gas, to be used as γ_{air} in (7)	Experimental p_2, kPa [5]	Solution (7),(11)-(13) this study		Solution by Boyack *et al*. [10] as developed in this study	
								p_2, kPa	error, %	p_2, kPa	error, %
CO2	0.4686	105.5	794.3	1.372	0.5314	1.289	295.7	402.1	36.0	431.8	46.0
CO2	0.8783	109.3	794.3	1.372	0.1217	1.289	491.9	701.1	42.5	711.9	44.7
He	0.4686	105.4	794.3	1.372	0.5314	1.667	335.8	428.7	27.7	456.8	36.0
He	0.8783	105.8	794.3	1.372	0.1217	1.667	553.1	710.1	28.4	719.8	30.1
N2	0.4686	104.7	794.3	1.372	0.5314	1.4	316.5	409.8	29.4	439.1	38.7
N2	0.8783	109.8	794.3	1.372	0.1217	1.4	530.1	704.2	32.8	714.6	34.8

Table 2. Solution of the model equations (7), (11)-(13) for (p_2-p_0)=10 kPa.

φ	Φ	p_{b1}, Pa	T_{b1}, K	$x_{H2} = \varphi \cdot \Phi$
0.04	0.0786	$2.46 \cdot 10^5$	720.5	$3.14 \cdot 10^{-3}$
0.08	0.0474	$3.59 \cdot 10^5$	1074.5	$3.79 \cdot 10^{-3}$
0.12	0.0355	$4.59 \cdot 10^5$	1404.5	$4.26 \cdot 10^{-3}$
0.16	0.0293	$5.50 \cdot 10^5$	1718.0	$4.69 \cdot 10^{-3}$
0.20	0.0253	$6.32 \cdot 10^5$	2020.0	$5.06 \cdot 10^{-3}$

3 Vented deflagration of localised homogeneous and inhomogeneous mixture

3.1 Experimental programme

3.1.1 Experiments at Karlsruhe Institute of Technology (KIT)

Experimental compaign on vented deflagrations with uniform and stratified hydrogen-air mixtures was conducted at KIT as a part of coherent effort withon HyIndoor project [28]. The vented vessel at KIT had nearly cubic shape with dimensions $H \times W \times L$=1000×960×980 mm and is shown in Figure 2a. The vessel was located in a room having sizes 5.5×8.5×3.4 m and 160 m^3 volume (see Figure 2b). Rear, bottom and front panels were manufactured of 10 mm thick aluminium plate. The top, left and right vessel walls were fabricated of optically transparent sandwich panels (5 mm thick fire-resistant glass and 15 mm thick plexiglass on the outer side) to provide optical access and video record of deflagration process. Background Oriented Schlieren (BOS) technique was used to detect flame front location based on visualisation of density gradients, for which a random background pattern was fixed behind the experimental vessel seen in Figure 2b. The vent was sealed using stretched latex membrane for the duration of mixture preparation procedure. To avoid effect of membrane on deflagration dynamics, it was cut open using electrically driven knife prior to ignition.

The experiments with uniform (homogeneous) hydrogen-air flammable layers are summarised in Table 3, and experiments with non-uniform (inhomegeneous) hydrogen-air mixtures – in Table 4. The experimental programme with uniform concentration layers included hydrogen volumetric fractions in air φ =0.10, 0.15, 0.20 and 0.25, and unburnt mixture volume fractions in the enclosure Φ=0.25 and 0.50. A square vent of the same area 0.25 m^2 was used in all experiments with uniform mixtures. Experiments with non-uniform layers included six different gradient layers with maximum hydrogen fraction under the ceiling from φ=0.10 to φ=0.20, and a vent with area either 0.01 m^2 or 0.25 m^2. Details of hydrogen distribution in non-uniform layer experiments are given in the following section.

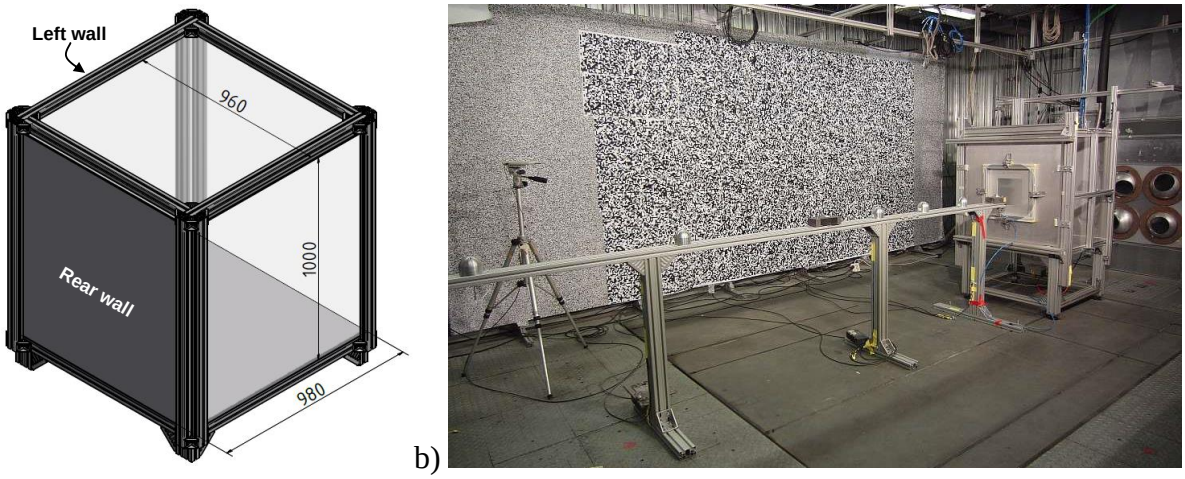

Figure 2. KIT experimental facility: a) test vessel design, b) test vessel (front view) inside the facility room.

Hydrogen-air mixture with specified hydrogen concentration was prepared using flows of hydrogen and air via mass flow Bronkhorst type controllers with an accuracy of ± 0.1% H_2 vol. For this, the streams of hydrogen and air were mixed in a mixing chamber outside of the test vessel, and then this homogenous mixture was slowly brought into the vessel close to the top plate. Thickness of the layer was controlled adjusting the height of the exhaust pipe, which was used to evacuate displaced gases. Hydrogen concentration in the vessel and in the exhaust flow was continuously monitored, and the specified layer of

given hydrogen-air mixture was formed when hydrogen concentration at outflow reached that one at the inflow. Hydrogen concentration was monitored during mixture preparation by sampling probes method combined with Fisher-Rosemount MLT4 gas analyser. The accuracy of concentration measurements in a stratified layer was ±0.2% H_2 vol. at certain position. The spatial non-uniformity of hydrogen concentration at different horizontal position of the same vertical coordinate was evaluated for four points and was within ±0.3% H_2 vol.

Fast PCB pressure transducers, Kistler and Kulite XTEX pressure sensors were used to measure experimental overpressure: four transducers inside the vessel and five transducers outside of it, two sensors inside and two sensors outside the vessel. Pressure dynamics was recorded using a fast data acquisition system. The accuracy of pressure measurements was within ±5% depending on the signal level. Pressure signal was processed using the Fast Fourier Transformation (FFT) with a low band filter of 400 Hz to exclude an effect of acoustic noise and filter out oscillations associated with natural frequency of the enclosure, improving pressure measurements accuracy to ±2%.

Ignition system used spark electrodes with continuous sparking for reliable ignition and allowed to ignite the mixture in various vessel locations. The ignition electrodes for all experiments with uniform and non-uniform hydrogen-air layers were located in the enclosure centre-plane, at distance 25 mm from the rear wall and 25 mm from the ceiling.

Table 3. Details of hydrogen-air uniform layer deflagration experiments in KIT facility.

Experiment	Volumetric fraction of flammable mixture in the vessel, Φ	Hydrogen volumetric fraction in the flammable mixture, φ	Vent area, m^2	Maximum overpressure, Pa
HIWP3-072	0.25	0.10	0.25	107.8
HIWP3-073	0.50	0.10	0.25	240.1
HIWP3-074	0.25	0.15	0.25	452.3
HIWP3-075	0.50	0.15	0.25	1427.0
HIWP3-076	0.25	0.20	0.25	2656.4
HIWP3-077	0.25	0.20	0.25	2581.1
HIWP3-078	0.50	0.20	0.25	6273.0
HIWP3-079	0.25	0.25	0.25	6257.4
HIWP3-081	0.50	0.20	0.25	7900.3
HIWP3-082	0.50	0.25	0.25	18339.1

Table 4. Details of hydrogen-air non-uniform layer deflagration experiments in KIT facility.

Experiment	Mixture gradient (min-max hydrogen fraction in mixture φ, vol.)	Vent area, m^2	Maximum overpressure, Pa
HIWP3-032	Gradient 6 (0.05-0.10)	0.01	350
HIWP3-033	Gradient 1 (0.02-0.12)	0.01	840
HIWP3-034	Gradient 2 (0.04-0.15)	0.01	2170
HIWP3-035	Gradient 3 (0.04-0.17)	0.01	2580
HIWP3-036	Gradient 3 (0.04-0.17)	0.01	2400
HIWP3-037	Gradient 4 (0.06-0.17)	0.01	2550
HIWP3-038	Gradient 5 (0.04-0.20)	0.01	3090
HIWP3-041	Gradient 3 (0.04-0.17)	0.01	2100
HIWP3-042	Gradient 3 (0.04-0.17)	0.01	3030
HIWP3-043	Gradient 4 (0.06-0.17)	0.01	2960
HIWP3-044	Gradient 2 (0.04-0.15)	0.01	2870
HIWP3-045	Gradient 6 (0.05-0.10)	0.25	48
HIWP3-046	Gradient 1 (0.02-0.12)	0.25	35
HIWP3-047	Gradient 2 (0.04-0.15)	0.25	52

Figure 3 gives two examples of flame propagation dynamics in a non-uniform mixture deflagration in experiments HIWP3-045 and HIWP3-072. Photos are taken from a side of the facility, the vent is on facility's left-hand side. Figure 3a shows initial stage of flame propagation with flame located at the rear of the facility under the ceiling. The flame propagation is predominantly in a horizontal direction along the flammable layer, Figure 3b. Figure 3c shows venting of combustion products. The products occupied the upper part of the facility. In experiment HIWP3-045 the products occupied relatively large part of the vent, while in HIWP3-072 the products were vented only through the upper part of the vent.

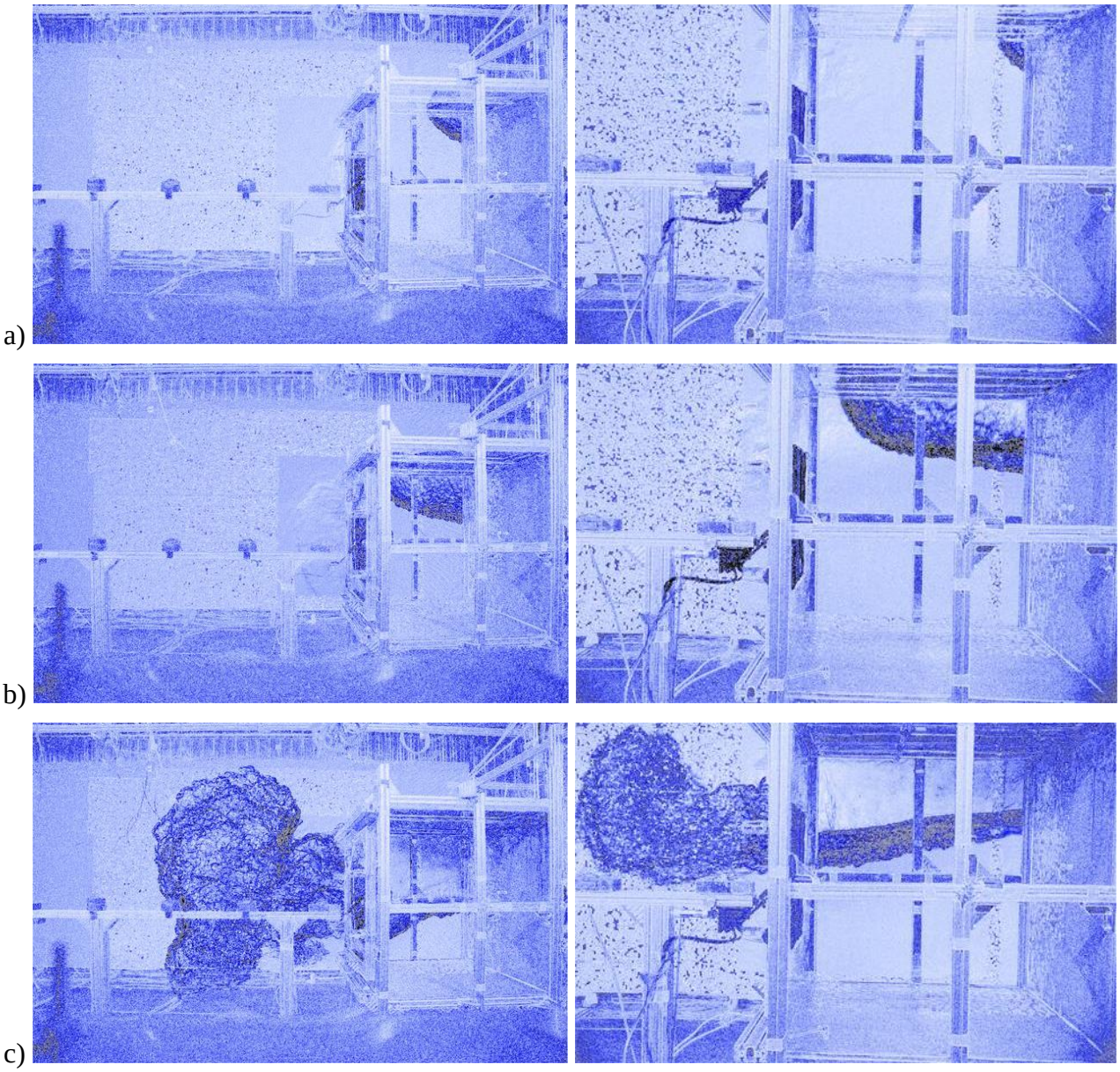

Figure 3. Deflagration propagation dynamics for tests HIWP3-045 (left) and HIWP3-072 (right): a) initial stage of flame propagation after ignition, b) further flame propagation in a layer within the vessel, c) venting of combustion products outside the vessel.

3.1.2 Experiments at Health and Safety Executive (HSE)

A series of large-scale tests on non-uniform mixture layers was conducted at the HSE facility (shown in Figure 4) as a part of HyIndoor project experimental work [24] and included uniform compositions as well. The vented enclosure has a geometry similar to many ISO container-based hydrogen facilities with dimensions; $H \times W \times L$ =2.5×2.5×5.0 m and internal volume of approximately 31 m^3. The enclosure was

located at the HSE test site in Buxton, fitted with passive vents and a flow controlled hydrogen supply. It was designed to withstand an internal overpressure of 0.2 bar. The hydrogen was introduced via a vertical pipe installed near the floor with a nominal release rate of 150 NL/min. A small hole in the floor was used to avoid over-pressurising the enclosure during the hydrogen release. For the considered experiments with non-uniform mixture layers the deflagrations were vented through passive vents 1 and 5 within the enclosure walls (see Figure 4b) each having an area of 0.224 m^2. The vents were covered by 20 micrometers polyethylene sheet pre-perforated around its perimeter to facilitate "clean" opening during a deflagration. This arrangement typically gave an opening pressure of approximately 1 kPa for the vent covers. The mixtures were ignited by a spark plug located at 0.3 m distance from the ceiling and 0.8 m from the far wall opposite to the vents 1 and 5. The ignition source was an AC spark, which ran for a few seconds and provided relatively large ignition energy (in excess of 1 J). The hydrogen concentration was analysed by measuring the change in oxygen concentration depletion using electrochemical oxygen sensors, spaced at approximately 0.31 m from each other. Oxygen sensors had accuracy ±0.1% vol. in air, which translated to a hydrogen concentration uncertainty of ≈0.5% vol. The internal pressure was measured using two Kistler pressure transducers ranged 0–2 bar abs., which were mounted flush with the side walls of the enclosure.

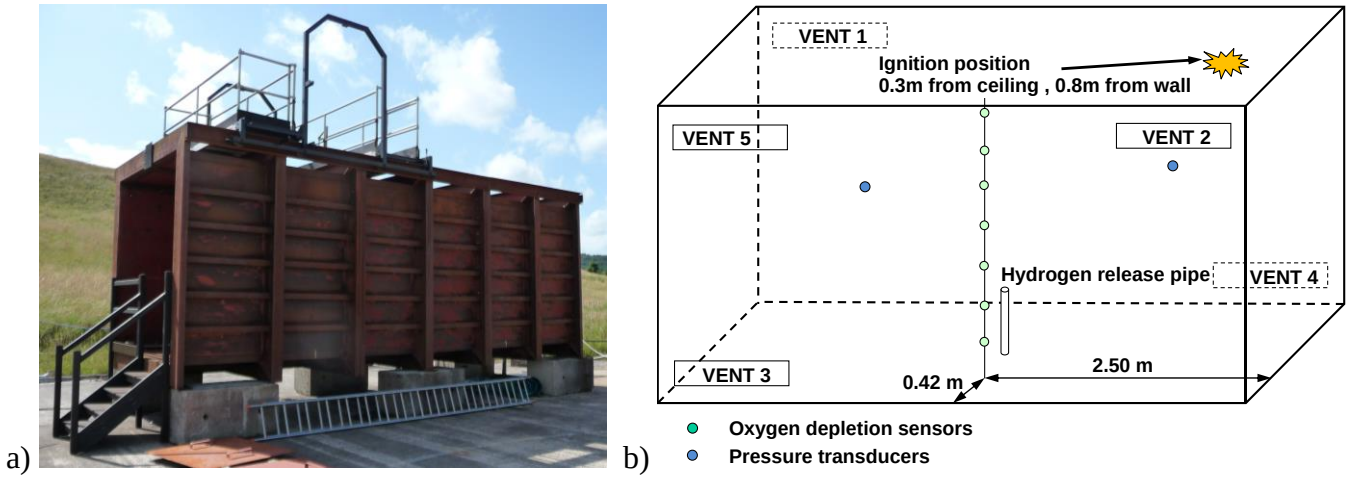

Figure 4. HSE experimental facility: a) test vessel view, b) test vessel scheme.

Three tests were conducted with stably stratified quiescent gradient mixtures in the HSE facility and are summarised in Table 5. The tests WP3/Test21 and WP3/Test26 had maximum deflagration overpressure equal to the vent opening overpressure, i.e. maximum overpressure was not result of deflagration dynamics at the end of the process but merely determined by strength of polyethylene cover. By this reason these tests are not used for the model validation and only test WP3/Test22 is part of the model validation domain.

Table 5. Details of hydrogen-air non-uniform layer deflagration experiments in HSE facility.

Experiment	Min-max hydrogen fraction in the flammable mixture, φ	Vent area, m^2	Vent burst overpressure, kPa	Maximum overpressure, kPa
WP3/Test21	0.001-0.105	0.448	2	2
WP3/Test22	0.001-0.123	0.448	1	5
WP3/Test26	0.001-0.101	0.448	2.5	2.5

3.2 Theoretical model

3.2.1 Major derivation steps and assumptions

Figure 5a shows a schematic physical layout for localised mixture deflagration in a vented enclosure at initial moment: a layer of flammable fuel-air mixture is located under the ceiling of the enclosure. Figure 5b demonstrates a conceptual calculation scheme corresponding to the same arrangement and used for the

model development: the flammable mixture contains fuel of mass m_f occupying volume V_f, and air with mass m'_{air} occupying volume V'_{air}. Total mass of air in the enclosure, including air in flammable mixture, is m_{air} and total air volume is V_{air}. It makes volumetric fraction of fuel in the flammable mixture $\varphi = V_f / (V_f + V'_{air})$, and fraction of flammable mixture in the vessel volume $\Phi = (V_f + V'_{air})/(V_f + V_{air})$.

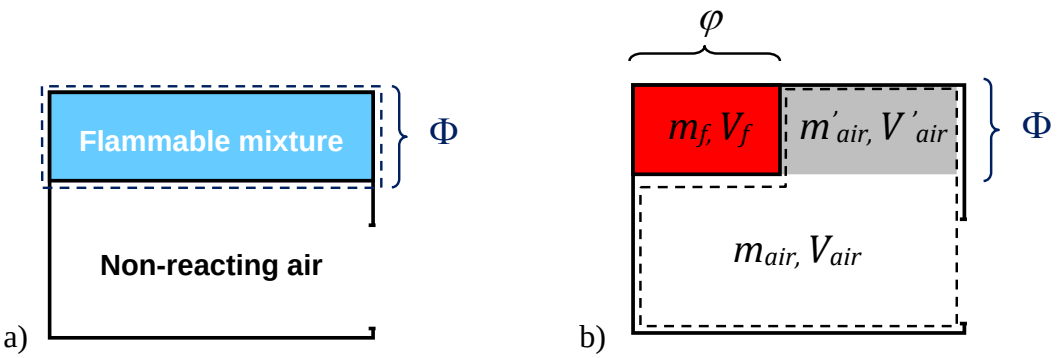

Figure 5. Localised flammable mixture in a vented enclosure: a) layout, b) calculation scheme.

The background of the localised vented deflagration model was suggested for the first time in 1996 by one of the authors [33]. Its major derivation steps are based on the vented deflagration model for uniform flammable mixture occupying the entire enclosure volume [14]. The model is built on the volume conservation equation in the enclosure written in non-dimensional form for burnt and unburnt mixture (the last includes both flammable mixture and non-reacting air)

$$\omega_b + \omega_u = 1, \tag{16}$$

includes the equation for mass flow rate for sub-sonic release through the vent

$$G = \mu F \left\{ \frac{2\gamma}{\gamma - 1} \rho\, p \left(\frac{p_i}{p} \right)^{2/\gamma} \left[1 - \left(\frac{p_i}{p} \right)^{(\gamma-1)/\gamma} \right] \right\}^{0.5}, \tag{17}$$

the non-dimensional mass conservation equation for burnt and unburnt mixtures

$$n_b + n_u + \int_0^t \left[\frac{A G_b + (1-A) G_u}{m_i} \right] dt = 1, \tag{18}$$

and the non-dimensional equation for conservation of internal energy

$$u_i = \int_{n_b} u_b\, dn_b + \int_{n_u} u_u\, dn_u + \int_0^t \left[A \left(u_b + \frac{p}{\rho_b} \right) \frac{G_b}{m_i} + (1-A) \left(u_u + \frac{p}{\rho_u} \right) \frac{G_u}{m_i} \right] dt\,. \tag{19}$$

The internal energy of unburnt and burnt mixtures can be written respectively as:

$$u_u = u_i + \frac{c_{vu}}{M_u} (T_u - T_{ui}), \quad u_b = u_i + \frac{c_{vb}}{M_b} (T_b - T_{bi}) - R \left(\frac{T_{bi}}{M_b} - \frac{T_{ui}}{M_u} \right). \tag{20}$$

It can be shown that $\sigma_b = \frac{\rho_b}{\rho_i} = \frac{m_b}{V_b} \frac{V}{m} = \frac{n_b}{\omega_b} = \frac{n_b}{1-\omega_u} = \frac{n_b}{1-(n_u/\sigma_u)} = \frac{n_b \sigma_u}{\sigma_u - n_u}$. Using this equation, the perfect gas law and the adiabatic expansion/compression assumptions, an expression for non-dimensional pressure can be derived:

$$\sigma_u^{\gamma_u} = \left(\frac{\rho_u}{\rho_{ui}} \right)^{\gamma_u} = \frac{p}{p_i} = \pi = \frac{\rho_b\, n_b\, R T_b}{\rho_i\, n_{ui}\, R T_{ui}} = \frac{(\rho_b/\rho_{bi})(T_b/M_b) n_b}{T_{ui}/M_{ui}} = \frac{\sigma_b (T_b/M_b) n_b}{T_{ui}/M_{ui}}, \tag{21}$$

from which it follows that

$$\frac{T_b}{M_b} n_b = \frac{T_{ui}}{M_{ui}} \sigma_u^{\gamma_u - 1} \frac{\sigma_u - n_u}{n_b} . \tag{22}$$

Using thermodynamic relations for adiabatic process $\gamma - 1 = R/c_v$, $T_u / T_{ui} = \pi^{1-1/\gamma_u}$, and the definition of the combustion products expansion coefficient $E_i = M_u T_{bi} / M_b T_{ui}$, the energy conservation equation becomes:

$$\pi + \gamma_b - 1 = \gamma_b E_i \left(n_b + \int_0^t \frac{A G_b}{m_i} dt \right) + \frac{\gamma_b - \gamma_u}{\gamma_b - 1} \pi^{1-1/\gamma_u} n_u + \tag{23}$$

$$+ \gamma_u \frac{\gamma_u - \gamma_b}{\gamma_u - 1} \left[n_u + \int_0^t (1-A)\left(1 - \pi^{1-1/\gamma_u}\right) \frac{G_u}{m_i} dt \right] - \gamma_b \int_0^t A \pi^{1-1/\gamma_u} \frac{\left(\pi^{1/\gamma_u} - n_u\right)}{n_b} \frac{G_b}{m_i} dt .$$

This equation does not contain the burning velocity yet, which may be introduced via the dimensionless mass conservation equations for burnt and unburnt gas respectively:

$$\frac{dn_b}{d\tau} = 3\left[\chi \pi^{\varepsilon + 1/\gamma_u} \left(1 - n_u \pi^{-1/\gamma_u}\right)^{2/3} + (1-A) R_b^{\#} W \right], \tag{24}$$

$$\frac{dn_u}{d\tau} = -3\left[\chi \pi^{\varepsilon + 1/\gamma_u} \left(1 - n_u \pi^{-1/\gamma_u}\right)^{2/3} + (1-A) R_u^{\#} W \right], \tag{25}$$

where $R_u^{\#}$, $R_b^{\#}$ are non-dimensional parameters equal respectively to:

$$R_u^{\#} = \left\{ (2\gamma_u)/(\gamma_u - 1) \pi \sigma_u \left[(1/\pi)^{2/\gamma_u} - (1/\pi)^{1+1/\gamma_u} \right] \right\}^{1/2}, \tag{26}$$

$$R_b^{\#} = \left\{ (2\gamma_b)/(\gamma_b - 1) \pi \sigma_b \left[(1/\pi)^{2/\gamma_b} - (1/\pi)^{1+1/\gamma_b} \right] \right\}^{1/2}, \tag{27}$$

and W is the venting parameter, which may be expressed via the turbulent Bradley number, Br_t, as:

$$W = \frac{1}{(36\pi_0)^{1/3} \sqrt{\gamma_u}} \frac{\mu F}{V^{2/3}} \frac{c_{ui}}{S_{ui}} = \left(\frac{\sqrt{E_i / \gamma_u}}{(36\pi_0)^{1/3}} \frac{\mu}{\chi} \frac{F}{V^{2/3}} \frac{c_{ui}}{S_{ui}(E_i - 1)} \right) \left(\frac{\chi (E_i - 1)}{\sqrt{E_i}} \right) = Br_t \frac{\chi (E_i - 1)}{\sqrt{E_i}} . \tag{28}$$

Then, the energy conservation equation gives a pressure dynamics equation in dimensionless form:

$$\frac{d\pi}{d\tau} = \frac{\chi Z \pi^{(\varepsilon+1)/\gamma_u} \left(1 - n_u \pi^{-1/\gamma_u}\right)^{2/3} - \gamma_b W \left[(1-A) R_u^{\#} + A R_b^{\#} \frac{\pi^{1/\gamma_u} - n_u}{n_b} \right]}{\left(\pi^{1/\gamma_u} - \frac{\gamma_u - \gamma_b}{\gamma_u} n_u \right) \frac{1}{3\pi}} , \tag{29}$$

where

$$Z = \gamma_b \left[E_i - \frac{\gamma_u}{\gamma_b} \frac{\gamma_b - 1}{\gamma_u - 1} \right] \pi^{(1-\gamma_u)/\gamma_u} + \frac{\gamma_u - \gamma_b}{\gamma_u - 1} .$$

The two members in the numerator of the RHS of this equation are responsible for the "competition" between pressure increase due to combustion process (positive member) and pressure decrease due to outflow of gases through the vent (negative member).

The further model development is done for low-strength equipment and buildings when the dimensionless overpressure can be accepted as $\Delta\pi < 1$. The model assumptions are:

1. The maximum overpressure is achieved when $\partial\pi / \partial\tau = 0$, hence we can assume that the numerator in equation (29) is equal to zero, and thus:

$$\chi Z \pi^{(\varepsilon+1)/\gamma_u} \left(1 - n_u \pi^{-1/\gamma_u}\right)^{2/3} = \gamma_b W \left[(1-A) R_u^{\#} + A R_b^{\#} \left(\frac{\pi^{1/\gamma_u} - n_u}{n_b} \right) \right]. \tag{30}$$

Once by the definition $\sigma_u = \pi^{1/\gamma_u}$ and $\omega_u = n_u / \sigma_u$, then

$$\chi Z \pi^{(\varepsilon+1)/\gamma_u} \omega_b^{2/3} = \gamma_b W \left[(1-A) R_u^{\#} + A R_b^{\#} \left(\frac{\pi^{1/\gamma_u} - n_u}{n_b} \right) \right]. \tag{31}$$

2. In many cases a localised flammable mixture will be far from the vent due to the fact that it occupies only a fraction of the enclosure volume. This assumption is conservative from safety point of view since the outflow of combustion products decreases deflagration overpressure more efficiently compared to the outflow of unburnt gas (because the higher outflowing gas temperature the higher outflow volumetric flow rate). Then, we can assume that the outflowing gas is entirely the unburnt mixture, i.e. there is no combustion products in the vent and thus the model parameter $A = 0$. This results in the simplication of equation (31) to:

$$\chi Z \pi^{(\varepsilon+1)/\gamma_u} \omega_b^{2/3} = \gamma_b W R_u^{\#}. \tag{32}$$

3. For the purposes of this study with the reasonable accuracy we could assume $\gamma_b = \gamma_u = \gamma$, and thus:

$$\chi Z \pi^{(\varepsilon+1)/\gamma} \omega_b^{2/3} = \gamma W R_u^{\#}. \tag{33}$$

Hence, the venting parameter can be expressed as:

$$W = \frac{\chi Z \pi^{(\varepsilon+1)/\gamma} \omega_b^{2/3}}{\gamma R_u^{\#}}. \tag{34}$$

The same assumption $\gamma_b = \gamma_u = \gamma$ leads to an updated equation for parameter *Z*:

$$Z = \gamma_b \left[E_i - \frac{\gamma_u}{\gamma_b} \frac{\gamma_b - 1}{\gamma_u - 1} \right] \pi^{(1-\gamma_u)/\gamma_u} + \frac{\gamma_u - \gamma_b}{\gamma_u - 1} = \gamma \left[E_i - 1 \right] \pi^{(1-\gamma)/\gamma}. \tag{35}$$

4. At the end of combustion process the volume fraction of adiabatically compressed burnt products ω_b may be expressed using initial volume fraction of the flammable mixture ω_{mi}, expansion coefficient of combustion products at initial conditions E_i, and non-dimensional pressure as $\omega_b = \omega_{mi} E_i \pi^{-1/\gamma}$, and further, using the initial mass fraction of flammable mixture n_{mi}, as

$$\omega_b = \omega_{mi} E_i \pi^{-1/\gamma} = \left(\frac{n_{mi} / M_m}{\frac{n_{mi}}{M_m} + \frac{n_{air}}{M_{air}}} \right) E_i \pi^{-1/\gamma}. \tag{36}$$

The assumption $M_m \approx M_{air}$, reduces this further to $w_b \approx E_i n_{mi} \pi^{-1/\gamma}$. It should be underlined that due to dimensionless volume conservation equation (16) ω_b cannot exceed 1.0 (because volume of burnt mixture in an enclosure cannot be larger than the volume of enclosure itself). This step of development process represents the largest difference compare to the model for an enclosure fully filled with flammable mixture.

5. Equation (26) for $R_u^{\#}$ can be simplified if the function $f(\pi) = \left(\frac{1}{\pi} \right)^x$ is expanded in Taylor series about $\pi = 1$ as follows: $f(\pi) \approx f(1) + f'(1)(\pi - 1) + 0(\pi - 1)^2$, where $f(1) = (1/\pi)^x = (1/1)^x = 1$, $f'(\pi) = \left[(1/\pi)^x \right]' = \left[\pi^{-x} \right]' = -x \pi^{-x-1} = -x \pi^{-(x+1)}$. Hence, $f'(1) = -x (1)^{-(x+1)} = -x$, and the whole function may

be approximated as $f(\pi)=(1/\pi)^x \approx 1-x(\pi-1)$.

Then, the equation for $R_u^{\#}$ can be re-written in a simpler form as:

$$R_u^{\#}=\left\{\frac{2\gamma}{\gamma-1}\pi\sigma_u\left[\left(\frac{1}{\pi}\right)^{2/\gamma}-\left(\frac{1}{\pi}\right)^{(\gamma+1)/\gamma}\right]\right\}^{1/2}=\left\{\frac{2\gamma}{\gamma-1}\pi\sigma_u\left[\left(1-\frac{2}{\gamma}(\pi-1)\right)-\left(1-\frac{\gamma+1}{\gamma}(\pi-1)\right)\right]\right\}^{1/2}= \tag{37}$$

$$=\left\{\frac{2\gamma}{\gamma-1}\pi\sigma_u(\pi-1)\frac{\gamma-1}{\gamma}\right\}^{1/2}=\left\{2\pi(\pi-1)\sigma_u\right\}^{1/2}.$$

6. Using dimensionless density $\sigma_u=\pi^{1/\gamma}$, the equation for $R_u^{\#}$ can be rewritten as $R_u^{\#}=\left\{2\pi(\pi-1)\pi^{1/\gamma}\right\}^{1/2}$. Finally, substituting equations for ω_b, Z and $R_u^{\#}$ in equation (34) for W gives:

$$W=\frac{\chi\gamma(E_i-1)\pi^{(1-\gamma)/\gamma}\,\pi^{1/\gamma+\varepsilon}\left(E_i\,n_{mi}\,\pi^{-1/\gamma}\right)^{2/3}}{\gamma\left\{2\pi(\pi-1)\pi^{1/\gamma}\right\}^{1/2}}=\frac{\chi(E_i-1)\,E_i^{2/3}\,n_{mi}^{2/3}}{\left[2(\pi-1)\right]^{1/2}}\pi^{(1-\gamma)/\gamma}\,\pi^{\varepsilon+1/\gamma}\pi^{-2/3\gamma}= \tag{38}$$

$$=\frac{\chi(E_i-1)\,E_i^{2/3}\,n_{mi}^{2/3}}{\left[2(\pi-1)\right]^{1/2}}\pi^{(1-\gamma)/\gamma+1/\gamma+\varepsilon-2/3\gamma}=\frac{\chi(E_i-1)\,E_i^{2/3}\,n_{mi}^{2/3}}{\left[2(\pi-1)\right]^{1/2}}\pi^{\frac{5-9\gamma}{6\gamma}+\varepsilon}.$$

Table 6 demonstrates that for pressures, which are characteristic for low-strength equipment and buildings and lean hydrogen mixtures, the expression $\pi^{(5-9\gamma)/6\gamma+\varepsilon}$ is close to 1 with acceptable for engineering correlations accuracy.

Table 6. Value $\pi^{(5-9\gamma)/6\gamma+\varepsilon}$ for hydrogen-air mixtures.

Hydrogen fraction, φ	Overall thermodynamic index*, ε	Adiabatic index, γ	Non-dimensional pressure, π	Value $\pi^{(5-9\gamma)/6\gamma+\varepsilon}$
0.3	0.55	1.4	1.2	0.938
0.2	≈0.63	1.4	1.2	0.952
0.1	≈0.74	1.4	1.2	0.971

Note: * - see definition further in the text.

As a result, the venting parameter may be equated to:

$$W=\frac{\chi(E_i-1)\,E_i^{2/3}\,n_{mi}^{2/3}}{\left[2(\pi-1)\right]^{1/2}}, \tag{39}$$

where $(\pi-1)=\Delta\pi$ is the sought-out dimensionless overpressure, which can be written, using (28), as:

$$\Delta\pi=\frac{\left(\chi(E_i-1)\,E_i^{2/3}\,n_{mi}^{2/3}\right)^2}{2W^2}=\left(\frac{\chi(E_i-1)\,E_i^{2/3}\,n_{mi}^{2/3}}{\sqrt{2}\,W}\right)^2=\left(\frac{\chi(E_i-1)\,E_i^{2/3}\,n_{mi}^{2/3}}{\sqrt{2}\,Br_t\,\chi(E_i-1)/\sqrt{E_i}}\right)^2=\left(\sqrt{\frac{E_i}{2}}\,\frac{E_i^{2/3}\,n_{mi}^{2/3}}{Br_t}\right)^2. \tag{40}$$

The term $E_i^{2/3}\,n_{mi}^{2/3}$ is the approximate expression of $w_b^{2/3}$, which cannot be larger than 1.0. Thus, the more appropriate form of equation (40) is:

$$\Delta\pi=\left(\sqrt{\frac{E_i}{2}}\,\frac{1}{Br_t}\right)^2\cdot MIN\left\{1.0;\left(E_i^{2/3}\,n_{mi}^{2/3}\right)^2\right\}. \tag{41}$$

7. A few auxiliary equations should be derived to express mass fraction of fuel-air mixture n_{mi} using its volumetric fraction in the enclosure, Φ, and volume fraction of fuel in the localised fuel-air mixture, φ. First, mass of air in localised hydrogen-air mixture $m_{air}^{'}$ can be expressed using its volumetric fraction $(1-\varphi)$ in the flammable volume $V_m^{'}$, and the perfect gas law:

$$m_{air}^{'} = \frac{pM_{air}}{RT}(1-\varphi)V_m = \frac{pM_{air}}{RT}(1-\varphi)\left(V_f + V_{air}^{'}\right) = \frac{pM_{air}}{RT}(1-\varphi)\left(\frac{m_f RT}{M_f p} + \frac{m_{air}^{'} RT}{M_{air} p}\right), \tag{42}$$

which may be rearranged as:

$$m_{air}^{'} = \frac{M_{air}}{M_f}\frac{(1-\varphi)}{\varphi} m_f . \tag{43}$$

Then, the volume fraction of fuel in the whole enclosure volume, $\varphi\Phi = V_f/(V_f + V_{air})$, can be rewritten using mass fractions instead of volume fractions as:

$$\varphi\Phi = \frac{\left(\frac{m_f}{m_f + m_{air}}\right)\Big/ M_f}{\left(\frac{m_f}{m_f + m_{air}}\right)\Big/ M_f + \left(\frac{m_{air}}{m_f + m_{air}}\right)\Big/ M_{air}} = \frac{m_f / M_f}{m_f / M_f + m_{air} / M_{air}} = \frac{1}{1 + \frac{m_{air}}{m_f}\frac{M_f}{M_{air}}},$$

from which

$$\frac{m_{air}}{m_f} = \frac{M_{air}}{M_f}\left(\frac{1}{\Phi\varphi} - 1\right). \tag{44}$$

The mass fraction of flammable fuel-air mixture $n_{mi} = (m_f + m_{air}^{'})/(m_f + m_{air})$, can be rewritten using equation (43) for $m_{air}^{'}$ as:

$$n_{mi} = \frac{M_{air}(1-\varphi) + M_f \varphi}{M_f \varphi(m_{air}/m_f + 1)} = \frac{1 + \left(\frac{1}{\varphi} - 1\right)\frac{M_a}{M_f}}{1 + m_{air}/m_f}, \tag{45}$$

which, taking into account (44), gives:

$$n_{mi} = \frac{1 + \left(\frac{1}{\varphi} - 1\right)\frac{M_{air}}{M_f}}{1 + \left(\frac{1}{\Phi\varphi} - 1\right)\frac{M_{air}}{M_f}}. \tag{46}$$

Thus, the equation for the dimensionless overpressure of localised flammable mixture vented deflagration is now:

$$\Delta\pi = \frac{\left(\chi\left(E_i - 1\right)\right)^2}{2\left(\frac{1}{\left(36\pi_0\right)^{1/3}\sqrt{\gamma}}\frac{\mu F}{V^{2/3}}\frac{c_{ui}}{S_{ui}}\right)^2} \cdot MIN\left\{1.0; \left[E_i^{2/3}\left(\frac{1+\left(\frac{1}{\varphi}-1\right)\frac{M_{air}}{M_f}}{1+\left(\frac{1}{\Phi\varphi}-1\right)\frac{M_{air}}{M_f}}\right)^{2/3}\right]^2\right\}, \quad (47)$$

or, bringing into consideration the turbulent Bradley number the theoretically derived correlation is:

$$\Delta\pi = \left(Br_t^{-1}\sqrt{\frac{E_i}{2}}\right)^2 \cdot MIN\left\{1.0; \left[E_i^{2/3}\left(\frac{1+\left(\frac{1}{\varphi}-1\right)\frac{M_{air}}{M_f}}{1+\left(\frac{1}{\Phi\varphi}-1\right)\frac{M_{air}}{M_f}}\right)^{2/3}\right]^2\right\}. \quad (48)$$

The correlation (48) will be adjusted to the experimental data in the form similar to the vented deflagration correlation for uniform mixtures occupying entire enclosure volume [4,19], i.e. $\Delta\pi = A\,Br_t^{-B}$ (theoretically derived coefficient B=2 will be tunned to reproduce experimental data):

$$\Delta\pi = A\,Br_t^{-B}\left(\sqrt{\frac{E_i}{2}} \cdot MIN\left\{1.0; \left[E_i^{2/3}\left(\frac{1+\left(\frac{1}{\varphi}-1\right)\frac{M_{air}}{M_f}}{1+\left(\frac{1}{\Phi\varphi}-1\right)\frac{M_{air}}{M_f}}\right)^{2/3}\right]\right\}\right)^2, \quad (49)$$

where the term in the paranthesis is "additional" compared to the venting correlation for deflagration of uniform mixture occupying the entire enclosure. In the limit $\Phi = 1$, the localised mixture vented deflagration overpressure (49) reduces to $\Delta\pi = A\,Br_t^{-B}\left(\sqrt{E_i/2}\right)^2$, which is marginally different from the uniform mixture correlation, i.e. $\Delta\pi = A\,Br_t^{-B}$ [4,19], due to peculiarities of the equation derivation along with the assumptions specific for localised mixture deflagrations. The value of coefficient B will be defined by back-fitting of the correlation to experimental data in section 3.5.

3.2.2 Flammable mixture properties

The laminar burning velocity of hydrogen-air mixture was calculated using equation $S_u = S_{u0}\left(\varphi_{H2}\right)\left(T/T_0\right)^m\left(p/p_0\right)^n$, where $S_{u0}\left(\varphi_{H2}\right)$ is the laminar burning velocity as a function of hydrogen volumetric fraction φ_{H_2} at initial temperature T_0 and pressure p_0, T and p are operating pressure and temperature, m and n are temperature and baric indexes respectively. For the ease of future correlation use an equation was developed for the burning velocity $S_{u0}\left(\varphi_{H2}\right)$ in the range $\varphi_{H2} = 0.12 - 0.20$ volumetric fraction based on the data [34]:

$$S_{u0}\left(\varphi_{H2}\right) = -4.7702\cdot10^4\varphi_{H2}^5 + 3.9615\cdot10^4\varphi_{H2}^4 - 1.3207\cdot10^4\varphi_{H2}^3 + 2.2392\cdot10^3\varphi_{H2}^2 - 1.8597\cdot10^2\varphi_{H2} + 6.02. \quad (50)$$

For hydrogen volumetric fraction equal to 0.10 reported in [34] burning velocity had a scatter between 0.070 and 0.115 m/s. The value closer to the upper measured value is adopted here: $S_{u0} = 0.11$ m/s. Below $\varphi_{H2} = 0.10$ burning velocities were taken from [35]. Temperature index m and baric index n were used as per [36], see Table 7.

Table 7. Temperature index, *m*, and baric index, *n*, as a function of hydrogen volume fraction, φ [36].

φ	0.15	0.20	0.25	0.295	0.35	0.40	0.43	0.45	0.50	0.55	0.60	0.65	0.70
m	2.6	2.2	1.9	1.7	1.5	1.45	1.4	1.4	1.45	1.5	1.7	1.9	2.2
n	-0.05	0.01	0.05	0.09	0.1	0.1	0.1	0.1	0.1	0.08	0.06	0.03	0

It is assumed that initial pressure in deflagration experiments is equal to the initial pressure at which burning velocity was measured, i.e. $(p_i/p_0)^n = 1.0$. The approximation for temperature index, *m*, is:

$$m = -25.94559 \cdot \varphi_{H2}^5 + 67.1521 \cdot \varphi_{H2}^4 - 66.6992 \cdot \varphi_{H2}^3 + 44.32819 \cdot \varphi_{H2}^2 - 18.5478 \cdot \varphi_{H2} + 4.5752 \,. \tag{51}$$

The dependence of combustion products expansion coefficient, E_i, on hydrogen fraction in the flammable mixture, φ, was calculated using thermodynamic equilibrium model and then approximated with the following correlation applicable for 0.04-0.34 hydrogen volumetric fraction range:

$$E_i(\varphi_{H2}) = 8.7755 \cdot 10^3 \varphi_{H2}^6 - 1.2712 \cdot 10^4 \varphi_{H2}^5 + 6.1677 \cdot 10^3 \varphi_{H2}^4 - 1.3646 \cdot 10^3 \varphi_{H2}^3 + \tag{52}$$

$$+ 8.7755 \cdot 10^3 \varphi_{H2}^6 + 1.2427 \cdot 10^2 \varphi_{H2}^2 + 19.767 \cdot \varphi_{H2} 1.1478 \cdot$$

3.2.3 Analysis of solution for dimensionless maximum vented deflagration overpressure $\Delta\pi$

The analytical solution for localised vented deflagration overpressure, equation (48), allows to analyse the effect of unburnt mixture fraction, Φ, and the fuel fraction in the flammable mixture, φ, on the maximum deflagration overpressure, $\Delta\pi$.

Expression in the brackets of RHS in correlation (48) contains the flammable mixture fraction Φ only in denominator of denominator and thus the whole expression should be approximately proportional to Φ. For the same flammable fuel-air composition the turbulent Bradley number Br_t will be the same. Hence, in the assumption that burnt mixture never exceeds the enclosure volume (i.e. neglecting *MIN* operator), from correlation (48) the maximum overpressure $\Delta\pi$ should be proportional to the flammable mixture volume fraction, Φ, in power 4/3.

For the same amount of released to enclosure fuel ($\Phi\varphi = Const$), the increase of the fuel fraction, φ, will result in the inversly proportional decrease of flammable mixture fraction, Φ. Then the ratio of deflagration overpressures achieved for two different mixtures with the same amount of released but differently dispersed fuel will be (at the moment we consider uniform fuel-air mixtures):

$$\frac{\Delta\pi_1}{\Delta\pi_2} = \left\{ \frac{S_{ui_1}\left(E_{i_1}-1\right)E_{i_1}^{2/3}}{S_{ui_2}\left(E_{i_2}-1\right)E_{i_2}^{2/3}} \frac{c_{ui_2}}{c_{ui_1}} \left(\frac{1+\left(\frac{1}{\varphi_1}-1\right)\frac{M_{air}}{M_f}}{1+\left(\frac{1}{\Phi_1\varphi_1}-1\right)\frac{M_{air}}{M_f}} \right)^{2/3} \Bigg/ \left(\frac{1+\left(\frac{1}{\varphi_2}-1\right)\frac{M_{air}}{M_f}}{1+\left(\frac{1}{\Phi_2\varphi_2}-1\right)\frac{M_{air}}{M_f}} \right)^{2/3} \right\}^2 . \tag{53}$$

The comparison of overpressure from deflagration of two different in fuel concentration localised hydrogen-air mixtures having the same amount of hydrogen in the same enclosure is given as an example in Table 8.

Table 8. Mixture properties for calculating overpressure ratio by equation (53).

Mixture	Φ	φ	S_{ui}, m/s	E_i	c_{ui}, m/s	$\Delta\pi_1/\Delta\pi_2$
1	0.1	0.2	0.862	5.52	381	112.4
2	0.2	0.1	0.117	3.50	361	

For the given choice of two mixtures, i.e. 20% of hydrogen in air for mixture "1", and 10% for mixture "2", and the theoretically obtained value of B=2 (see equations (48) and (49)), the deflagration overpressure ratio is significantly different, $\Delta\pi_1/\Delta\pi_2 = 112.4$. The increase of burning velocity, S_{ui}, and the expansion coefficient, E_i, for mixture "1" compared to mixture "2" has an overwhelming effect over the decrease of flammable mixture fraction, Φ. This example shows how serious implications could be if hydrogen safety system for indoor use is designed improperly.

This theoretical analysis indicates that the maximum overpressure in a localised vented deflagration will be strongly affected by a portion of mixture with the fastest burning velocity and the largest expansion coefficient, while contributions of slower burning parts of flammable mixture are expected to be negligible.

3.3 Deflagration-outflow interaction number, Ξ/μ

Calculation of the deflagration-outflow interaction (DOI) number (which may be thought as the overall flame wrinkling factor) to be used in the turbulent Bradley number, is done following the ideas of work [19]. The DOI number, Ξ/μ, is a product of individual flame wrinkling factors each responsible for different phenomena contributing to the increase of the burning rate: $\Xi/\mu = \Xi_K \Xi_{LP} \Xi_{FR} \Xi_{u'} \Xi_{AR} \Xi_O$. The model accounts currently for the following phenomena:

- dependence of laminar burning velocity on pressure and temperature of unburnt mixture;
- turbulence generated by flame front itself, Ξ_K;
- preferential diffusion in stretched turbulent flames (leading point concept), Ξ_{LP};
- fractal increase of flame front area, Ξ_{FR};
- flow turbulence in unburnt mixture, $\Xi_{u'}$;
- flame area increase due to elongation of flame in non-spherical vessel geometry, Ξ_{AR};
- flame turbulisation by obstacles, Ξ_O.

The flame wrinkling factors Ξ_K, Ξ_{LP}, Ξ_{FR}, $\Xi_{u'}$ are a legacy of CFD studies on modelling and large eddy simulations (LES) of hydrogen-air deflagrations carried out at Ulster during the last two decade and was successfully used to model deflagrations in a wide range of scales, environments and mixture compositions, see for example [37-44]. The state-of-the-art in the calculation of these wrinkling factors is described below.

The flame wrinkling factor due to turbulence generated by the flame front itself, Ξ_K, is based on the theory by Karlovits et al. [45]. The upper limit of this wrinkling factor, in the assumption that the turbulent burning velocity at high level of turbulence is close to u', was shown [46] to be equal to:

$$\Xi_K^{\max} = (E_i - 1)/\sqrt{3}. \tag{54}$$

Though the dependence of Karlovitz wrinkling factor on the flame radius was used in CFD simulations [19, 37-40,42-44], in the present lumped parameter model the dependence on the flame radius was relaxed and this wrinkling factor is taken equal to its maximum value following cited CFD studies:

$$\Xi_K = 1 + \left(\psi\, \Xi_K^{\max} - 1\right), \tag{55}$$

where ψ is the empirical coefficient reflecting the observation of the CFD study that the maximum value of the turbulence generated by the flame front itself was not realised all the time, probably because a turbulence level in the studied deflagration experiments didn't reach maximum value. The empirical coefficient ψ as a function of hydrogen volume fraction in the mixture φ is [19]:

$$\psi = 1 \qquad \text{for } \varphi < 0.2, \tag{56}$$

$\psi = -5\varphi + 2$ for $0.2 \le \varphi \le 0.3$,

$\psi = 0.5$ for $\varphi > 0.3$.

The leading point wrinkling factor Ξ_{LP} describes the increase of the burning rate due to the preferential diffusion in stretched flamelets of turbulent flames, which was named by Zeldovich as "leading points" effect. The combination of preferential diffusion and flame curvature provides the maximum burning rate for only a particular radius of curved flame from the spectrum of different radii in a turbulent brush. These points lead the propagation of turbulent combustion front. The wrinkling factor is calculated for different hydrogen concentrations following Zimont and Lipatnikov [47]. The CFD model [43, 44] presumes linear growth of leading point wrinkling factor with flame radius from unity to its maximum value approximated by equation (57). For the purpose of the correlation derivation Ξ_{LP} was taken equal to its maximum value because at the end of vented deflagration the combustion is turbulent. This wrinkling factor is approximated as a function of hydrogen volume fraction:

$$\Xi_{LP}^{\max} = 6.3\varphi_{H_2}^2 - 7.5\varphi_{H_2} + 3.0. \quad (57)$$

The wrinkling factor Ξ_{FR} accounts for combustion augmentation due to the increase of fractal surface of the flame front with its radius. Gostintsev et al. [48] concluded that the transition from laminar to fully turbulent self-similar regime of flame propagation occurs after critical flame radius, R_0. Here the flame wrinkling factor is calculated as [19]:

$$\begin{aligned} &\Xi_{FR} = 1.0 \text{ for } R \le R_0, \\ &\Xi_{FR} = \left(R/R_0\right)^{D-2} \text{ for } R > R_0, \end{aligned} \quad (58)$$

where the critical radius is calculated as a function of hydrogen volumetric fraction in a flammable mixture: $R_0 = 4.3478\,\varphi_{H_2} - 0.2826$ for $\varphi_{H_2} \le 0.295$ and $R_0 = 1.0$ m for $\varphi_{H_2} > 0.295$. This dependence is fitted to provide critical radius value $R_0 = 1.0$ m following conclusions of Gostintsev et al. [48], who reported the critical value $R_0 = 1.0 - 1.2$ m for near-stoichiometric hydrogen-air mixtures. The critical radius decreases in lean mixtures reflecting their higher susceptibility to thermo-diffusive instability. The fractal dimension value is adopted as $D = 2.33$ [49]. The calculation of fractal wrinkling factor (58) requires value of outer cut-off, *R*, which is taken as an enclosure size, i.e. $R = 1.0$ m for KIT tests and $R = 5.0$ m for the HSE experiment.

Wrinkling factor $\Xi_{u'}$ accounts for the effect of initial flow turbulence in unburnt mixture on flame propagation. Calculation of factor $\Xi_{u'}$ is based on RNG turbulence combustion model by Yakhot [50], realised here in a specific way (see [37-44] for details):

$S_t = \left(\Xi_K \Xi_{LP} \Xi_{FR} S_{u_i}\right) \cdot exp(u'/S_t)^2$,

so that turbulence wrinkling factor may be found as

$\Xi_{u'} = S_t / \left(\Xi_K \Xi_{LP} \Xi_{FR} S_{u_i}\right) = exp(u'/S_t)^2$.

In all considered validation experiments the mixture was initially quiescent ($u' = 0$) and the factor was taken as $\Xi_{u'} = 1.0$.

Premixed flame propagating through an enclosure tends to elongate towards a vent and take at the end of the process the shape of enclosure. The aspect ratio flame wrinkling factor, Ξ_{AR}, accounts for the growth of flame front area in non-spherical enclosure. It is calculated as the total area of the enclosure walls (total area of the flame envelope if local mixture combustion products do not occupy the entire enclosure volume) to the area of sphere having the same volume ("equivalent sphere") [4,17-19]. However, the combustion products may not occupy the whole enclosure for a localised deflagration, even if the entire localised

mixture is burnt, and the flame shape may be particularly elongated in non-uniform mixtures with fastest flame propagation along mixture composition with the largest burning velocity. This is the case for all non-uniform mixtures in KIT experiments (HIWP3-32 through to HIWP3-38, HIWP3-041 through to HIWP3-047), uniform mixture experiment HIWP3-072, and HSE experiment WP3/Test22. In this situation the aspect ratio wrinkling factor was calculated as the ratio of the area of total burnt mixture (occupying volume $\Phi E_i V$ under an enclosure ceiling), to the area of equivalent sphere having the same volume as expanded combustion products:

$$\Xi_{AR} = \frac{2\left[LW + \Phi E_i H\left(L+W\right)\right]}{\left[6\sqrt{\pi}\left(\Phi E_i V\right)\right]^{2/3}}. \qquad (59)$$

Flame wrinkling factor Ξ_O models flame acceleration due to wrinkling and turbulisation of the flame by obstacles. No obstacles were employed in the considered experimental program, and the factor was taken as $\Xi_O = 1.0$. There is data that this factor could be about 3-4 for "moderate" obstacles density in the case when enclosure fully filled in by flammable mixture. More research is needed to deeper undertstand and quantify the effect of obstacles in vented deflagration overpressure.

3.4 The model for non-uniform localised mixture vented deflagrations

The application of correlation (49) for venting of inhomogeneous localised mixture deflagration requires criteria for specification of a flammable layer volume fraction with highest burning velocity, which is responsible for the pressure build-up as demonstrated in section 3.2.3.

In this study the fraction of the fastest burning flammable mixture responsible for the pressure buildup, Φ^*, is calculated as a ratio of the flammable layer thickness, having the burning velocity within a specified range between the maximum burning velocity, $S_{u_{MAX}}$, which is located in stratified hydrogen-air mixture under the ceiling, and a fraction of this velocity, which has to be defined in this study, to the vessel height. The tested range of burning velocity was $\left(0.8-1.0\right)S_{u_{MAX}}$, $\left(0.9-1.0\right)S_{u_{MAX}}$, $\left(0.95-1.0\right)S_{u_{MAX}}$, and $\left(0.98-1.0\right)S_{u_{MAX}}$.

It was also assumed, based on the previous studies of the lower flammability limit on the direction of flame propagation, that the flame does not propagate downwards when hydrogen fraction in the mixture is below $\varphi_{H2} = 0.095$, and the flammable mixture fraction contributing to the pressure build-up, Φ, was limited by this threshold value as well.

Mixture properties (burning velocity, combustion products expansion coefficient, speed of sound, molecular mass) were calculated as a function of average hydrogen volumetric fraction in the considered portion of the layer responsible for the pressure build-up $\overline{\varphi}_{H_2} = \left(\varphi_{H_2 MAX} + \varphi_{H_2 MIN}\right)/2$. Hydrogen distribution with height in KIT and HSE experiments is given in Figure 6 and Figure 7 respectively. Numerical values of hydrogen fraction and burning velocity with height, and volume fraction of the fastest burning flammable mixtre Φ^* corresponding to the optimum range $\left(0.95-1.0\right)S_{u_{MAX}}$ (see section 3.5 below) are given for KIT experiments in Table 9, and for HSE experiment - in Table 10. Hydrogen concentrations in HSE experiment were measured only within heights 0.31-2.17 m, and concentration under the enclosure ceiling (height 2.50 m) was extrapolated preserving maximum measured hydrogen concentration value.

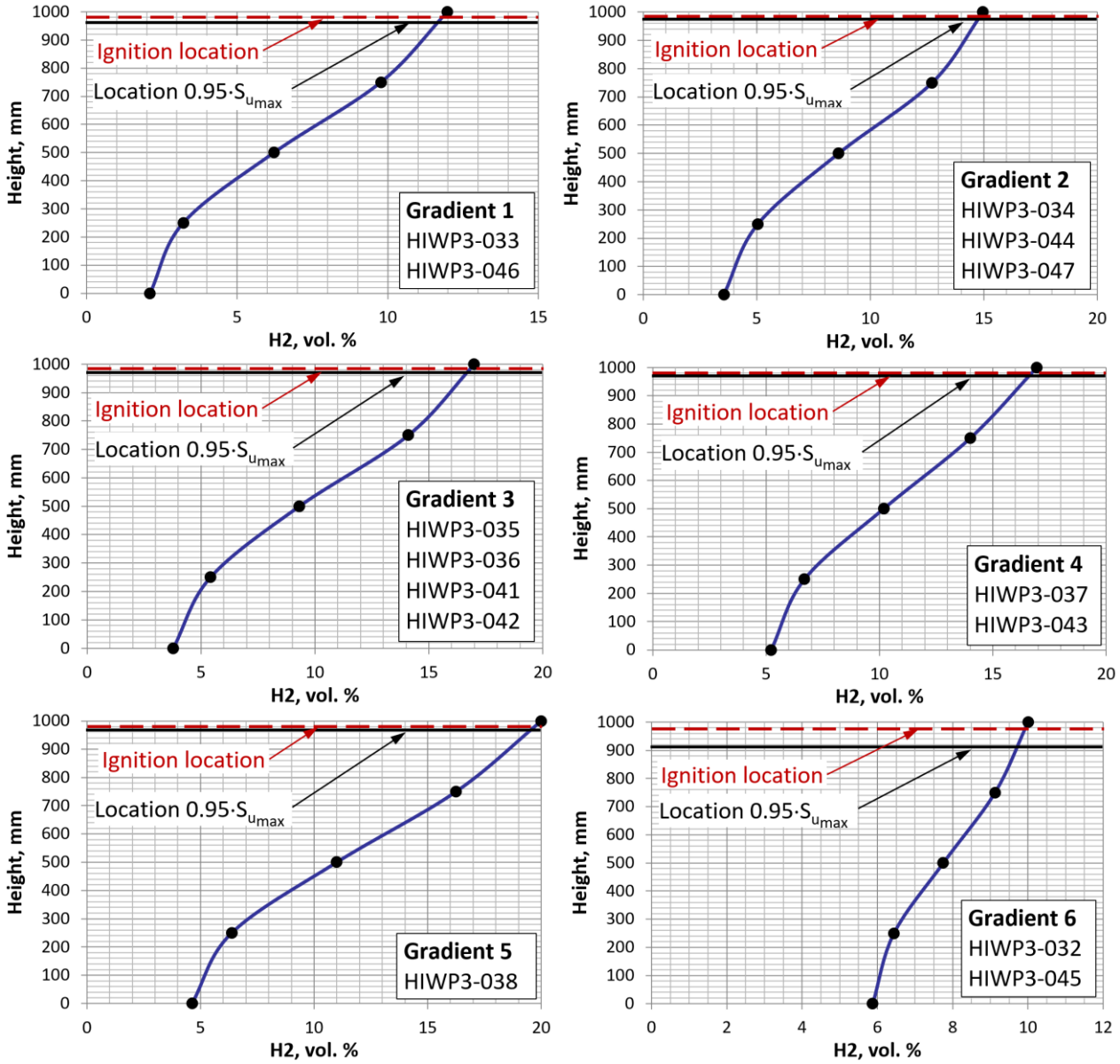

Figure 6. Hydrogen distribution with height in KIT experiments with inhomogeneous mixtures. Ignition location is 25 mm under the vessel ceiling.

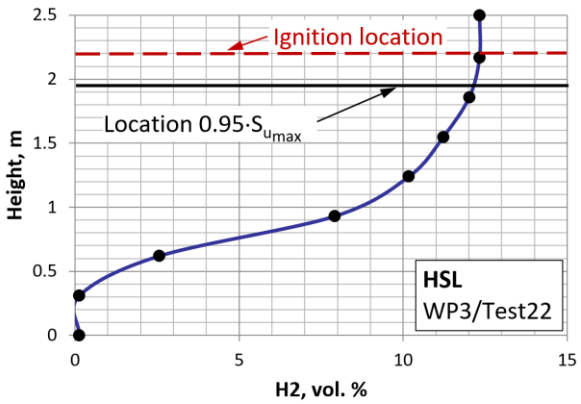

Figure 7. Hydrogen distribution with height in HSE test WP3/Test22 with inhomogeneous mixture. Ignition location is 0.30 m under the vessel ceiling.

Table 9. Mixture properties in KIT experiments (fraction of the fastest burning flammable mixture in the volume Φ^* is calculated for the burning velocity range $(0.95-1.0)S_{u_{MAX}}$).

	Gradient 1 (HIWP3-033, -046)			**Gradient 2** (HIWP3-034,-044,-047)			**Gradient 3** (HIWP3-035, -036, -041, -042)		
Height, m	H_2 volume fraction	Burning velocity S_u, m/s	Φ^*	H_2 volume fraction	Burning velocity S_u, m/s	Φ^*	H_2 volume fraction	Burning velocity S_u, m/s	Φ^*
1.00	0.1198	0.140	$3.71\cdot10^{-2}$	0.1495	0.362	$2.71\cdot10^{-2}$	0.1698	0.544	$2.708\cdot10^{-2}$
0.75	0.0987	0.093		0.1271	0.195		0.1409	0.292	
0.50	0.0623	0.051		0.0860	0.130		0.0931	0.100	
0.25	0.0321	0.0		0.0505	0.0		0.0541	0.047	
0	0.0211	0.0		0.0355	0.0		0.0377	0.0	
	Gradient 4 (HIWP3-037, -043)			**Gradient 5** (HIWP3-038)			**Gradient 6** (HIWP3-032, -045)		
Height, m	H_2 volume fraction	Burning velocity S_u, m/s	Φ^*	H_2 volume fraction	Burning velocity S_u, m/s	Φ^*	H_2 volume fraction	Burning velocity S_u, m/s	Φ^*
1.00	0.1694	0.540	$2.66\cdot10^{-2}$	0.2000	0.857	$2.81\cdot10^{-2}$	0.1000	0.100	$9.00\cdot10^{-2}$
0.75	0.1401	0.286		0.1625	0.475		0.0913	0.090	
0.50	0.1019	0.100		0.1100	0.125		0.0775	0.055	
0.25	0.0669	0.053		0.0638	0.052		0.0644	0.052	
0	0.0522	0.0		0.0463	0.0		0.0588	0.050	

Table 10. Mixture properties in HSE experiment WP3/Test22, burning velocity range $(0.95-1.0)S_{u_{MAX}}$.

Height, m	H_2 volume fraction	Burning velocity S_u, m/s	Φ^*
2.50	$0.1232^{\#}$	$0.172^{\#}$	$2.20\cdot10^{-1}$
2.17	0.1232	0.172	
1.86	0.1201	0.154	
1.55	0.1122	0.119	
1.24	0.1017	0.105	
0.93	0.0791	0.058	
0.62	0.0257	0.0	
0.31	0.0013	0.0	

Note: # - extrapolated value (equal to the maximum measured value).

3.5 The correlation and analysis of results

Data from KIT and HSE vented deflagration experiments with partially filled by flammable mixture enclosures were processed as described above. Coefficients *A* and *B* in the correlation (49) were obtained by fitting the calculated by correlation overpressures to experimental ones.

Four different ranges of the burning velocity were tested to define the needed fastest burning volume fraction, Φ^*, of a non-uniform flammable layer in the enclosure responsible for the pressure buid-up. The best results were obtained for the range $(0.95-1.0)S_{u_{MAX}}$. The widening of the range by the lower limit of burning velocities to $(0.8-1.0)S_{u_{MAX}}$ and $(0.9-1.0)S_{u_{MAX}}$ led to a larger value of Φ^*, higher overpressures in KIT non-uniform mixture experiments, and noticeable "departure" of uniform and non-uniform mixture overpressures from each other when correlated against the experimental data.

Contrary, the decrease of the burning velocity range to $(0.98-1.0)S_{u_{MAX}}$ led to too small value of the fatest burning flammable mixture fraction, Φ^*, and under-prediction of non-uniform layer vented deflagration overpressures with the same correlation coefficients, which again appeared as "departure" of predicted

uniform and non-uniform overpressures from each other but with non-uniform predictions now lower than uniform ones.

Table 11 shows values of Φ^*, the best-fit correlation coefficients *A* and *B*, and standard deviations between calculated by the correlation and experimental data for four tested ranges of burning velocities. The best agreement between experiments and the correlation (49) comprasing both uniform and non-uniform layers with flammable mixture fraction contributing to the maximum deflagration overpressure, Φ^*, corresponds to a relatively narrow range of burning velocity $(0.95-1.0)S_{u_{MAX}}$. This is in line with the result of the analysis of data in Table 8: deflagration overpressure is dominated by the fastest burning portion of a layer. Indeed, for the burning velocity range $(0.95-1.0)S_{u_{MAX}}$ the value of Φ^* in the most of considered experiments corresponds to 2.66% -3.71% of the enclosure volume, with the largest value in experiments with Gradient 6 mixtures (HIWP3-032, HIWP3-045, see Table 4), where flammable fraction of non-uniform layer contributing to the vented deflagration overpressure is 9% of the enclosure volume.

Table 11. Sensitivity of the correlation predictions to the burning velocity range.

	(0.80 – 1.0) $S_{u_{MAX}}$			(0.90 – 1.0) $S_{u_{MAX}}$			(0.95 – 1.0) $S_{u_{MAX}}$			(0.98 – 1.0) $S_{u_{MAX}}$		
	Φ^*, %	Best fit	St. dev., %	Φ^*, %	Best fit	St. dev., %	Φ^*, %	Best fit	St. dev., %	Φ^*, %	Best fit	St. dev., %
Grad.1	14.8	A=0.010, B=0.67	111.8	7.41	A=0.014, B=0.79	78.1	3.71	A=0.018, B=0.92	60.66	1.48	A=0.0320 B=0.99	63.1
Grad.2	10.9			5.43			2.71			1.09		
Grad.3	10.8			5.40			2.70			1.08		
Grad.4	10.6			5.32			2.66			1.06		
Grad.5	11.2			5.61			2.80			1.11		
Grad.6	14.3			1.43			9.00			1.00		
WP3/ Test22	13.0			6.96			22.0			1.39		

Figure 8 gives experimental, the best fit and conservative correlation overpressures versus parameter

$$Br_t^* = Br_t^{-B}\left(\sqrt{\frac{E_i}{2}}\cdot MIN\left\{1.0;\left[E_i^{2/3}\left(\frac{1+\left(\frac{1}{\varphi}-1\right)\frac{M_{air}}{M_f}}{1+\left(\frac{1}{\Phi\varphi}-1\right)\frac{M_{air}}{M_f}}\right)^{2/3}\right]\right\}\right)^2. \quad (60)$$

Filled and open symbols represent non-uniform and uniform mixtures respectively. The correlation (49) overpressures were calculated for the range $(0.95-1.0)S_{u_{MAX}}$. The best fit was obtained with the coefficients *A*=0.018 and *B*=0.92 using the least square method. The conservative correlation (to compensate for under-prediction in HIWP3-082 test) is achieved with coefficients *A*=0.080 and *B*=0.92, making conservative correlation overpressure 4.4 times larger than that obtained from the best fit.

The exact values of experimental and calculated overpressures are shown in Table 12 along with mixture properties and other calculated parameters. Experiments with non-uniform layered mixtures (Table 12, entries 1-14 and 25) are shaded by grey colour for easier identification.

The largest experimental overpressures in uniform layers, in agreement with the analysis of data in Table 8, are achieved for deflagrations with largest hydrogen concentrations: 25% by volume (HIWP3-079 and -082) and 20% by volume (HIWP3-076, -077, -078, -081) as expected.

For non-uniform mixture deflagrations the largest overpressures are also achieved in experiments where hydrogen concentrations under the ceiling are the largest: 20% vol. (HIWP3-038), 17% vol. (HIWP3-035, 036, 037, 041, 0.42, 0.43), and 15% vol. (HIWP3-034, -044).

Figure 8 demonstrates that the uniform and the non-uniform localised vented deflagrations obey the same correlation and have a comparable scatter. The largest overprediction for non-uniform layers is 186% for the test HIWP3-032 (Φ^*=0.09, φ=0.10), and the largest underprediction is -39% for the test HIWP-044 (Φ^*=0.027, φ=0.15), giving difference between over- and underprediction 225%; standard deviation of experimental and predicted overpressure differences is 55.5%. For uniform layers the largest overprediction is 153% for the test HIWP3-074 (Φ=0.25, φ=0.15), and the largest underprediction is -77% for the test HIWP3-082 (Φ=0.50, φ=0.25), resulting in spread of error 230%; standard deviation of experimental and predicted overpressure differences is 66.4%. This is comparable with the scatter for vented deflagration correlations for enclosures fully occupied by flammable mixture.

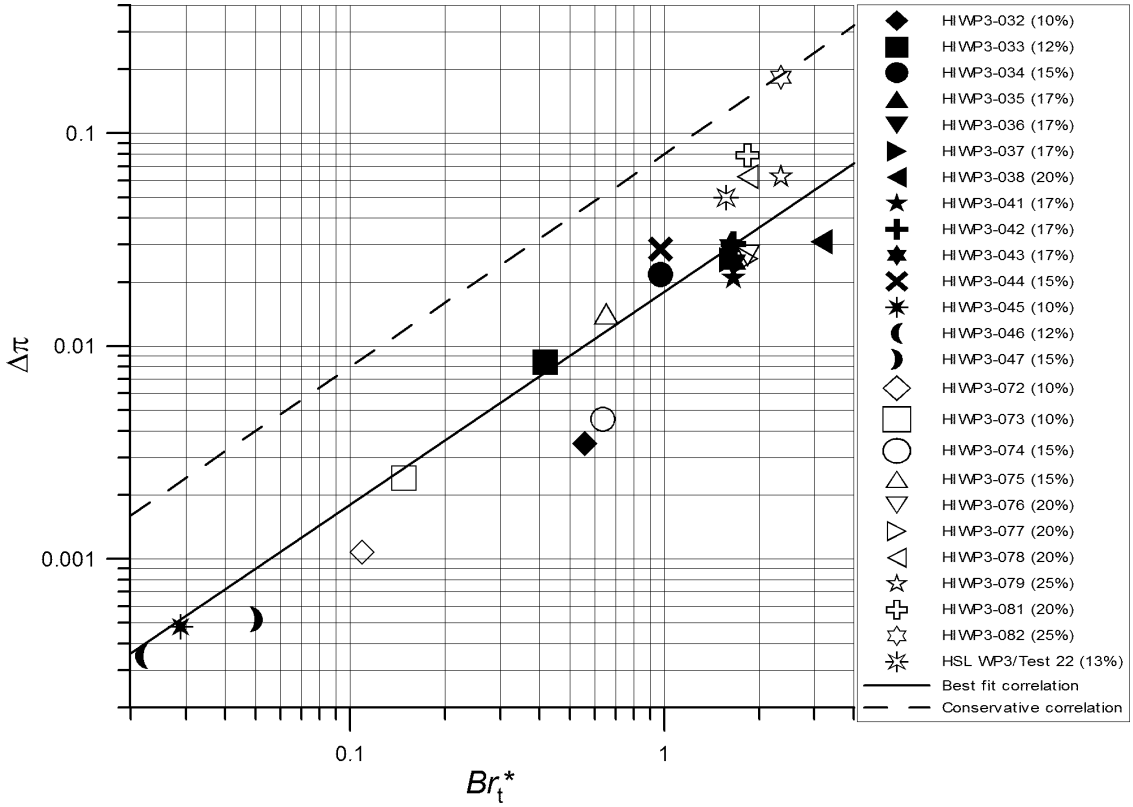

Figure 8. Comparison of experimental overpressure, and results of the best fit and conservative correlations (filled symbols – non-uniform mixtures, open symbols – uniform mixtures).

Figure 8 shows that the derived correlation reproduced the available set of 25 experiments in two different enclosures with reasonable engineering accuracy for a such complex phenomenon as vented deflagration of localised non-uniform and uniform mixture. A wider range of experimental conditions in terms of enclosure size, vent area, fraction of flammable uniform mixture in enclosure volume, Φ, fraction of flammable non-uniform mixture Φ^*, and hydrogen fraction in the mixture, φ, would help to further expand the validation domain of the correlation for localised vented deflagration derived here theoretically.

Table 12. Experimental versus best fit correlation (49) overpressures (A=0.018 and B=0.92).

	Experiment	Φ or Φ*, % (vol.)	$\overline{\varphi}$, % (vol.)	R_0, m	E_i	M_u, kg/kmol	S_{ui}, m/s	c_{ui}, m/s	Ξ_K	Ξ_{LP}	Ξ_{FR}	Ξ_{AR}	Ξ/μ	Br_t^{-1}	$\left(\frac{E_i}{\sqrt{2}}\right)^{1/2} MIN\{1.0; E_i^{2/3} n^{2/3}\}$	$\Delta\pi_{exp}$	$\Delta\pi_{corr}$
1	HIWP3-032	9.00	9.8	0.15	3.47	26.20	0.095	361	1.42	2.32	1.89	1.46	9.1	1.81	0.568	$3.50\cdot10^{-3}$	$1.00\cdot10^{-2}$
2	HIWP3-033	3.71	11.8	0.23	3.90	25.67	0.138	365	1.67	2.20	1.62	1.93	11.5	3.66	0.356	$8.40\cdot10^{-3}$	$7.52\cdot10^{-3}$
3	HIWP3-034	2.71	14.8	0.36	4.53	24.86	0.336	370	2.04	2.03	1.40	2.08	12.1	10.32	0.337	$2.17\cdot10^{-2}$	$1.75\cdot10^{-2}$
4	HIWP3-035	2.71	16.8	0.45	4.92	24.32	0.508	374	2.26	1.92	1.30	2.00	11.3	15.51	0.365	$2.58\cdot10^{-2}$	$2.98\cdot10^{-2}$
5	HIWP3-036	2.71	16.8	0.45	4.92	24.32	0.508	374	2.26	1.92	1.30	2.00	11.3	15.51	0.365	$2.40\cdot10^{-2}$	$2.98\cdot10^{-2}$
6	HIWP3-037	2.66	16.8	0.45	4.91	24.33	0.504	374	2.26	1.92	1.30	2.02	11.4	15.51	0.360	$2.55\cdot10^{-2}$	$2.91\cdot10^{-2}$
7	HIWP3-038	2.81	19.8	0.58	5.48	23.53	0.804	381	2.59	1.76	1.20	1.88	10.3	23.69	0.415	$3.09\cdot10^{-2}$	$5.69\cdot10^{-2}$
8	HIWP3-041	2.71	16.8	0.45	4.92	24.32	0.508	374	2.26	1.92	1.30	2.00	11.3	15.51	0.365	$2.10\cdot10^{-2}$	$2.98\cdot10^{-2}$
9	HIWP3-042	2.71	16.8	0.45	4.92	24.32	0.508	374	2.26	1.92	1.30	2.00	11.3	15.51	0.365	$3.03\cdot10^{-2}$	$2.98\cdot10^{-2}$
10	HIWP3-043	2.66	16.8	0.45	4.91	24.33	0.504	374	2.26	1.92	1.30	2.02	11.4	15.51	0.360	$2.96\cdot10^{-2}$	$2.91\cdot10^{-2}$
11	HIWP3-044	2.71	14.8	0.36	4.53	24.86	0.336	370	2.04	2.03	1.40	2.08	12.1	10.32	0.337	$2.87\cdot10^{-2}$	$1.75\cdot10^{-2}$
12	HIWP3-045	9.00	9.8	0.15	3.47	26.20	0.095	361	1.42	2.32	1.89	1.46	9.1	0.07	0.568	$4.80\cdot10^{-4}$	$5.19\cdot10^{-4}$
13	HIWP3-046	3.71	11.8	0.23	3.90	25.67	0.138	365	1.67	2.20	1.62	1.93	11.5	0.15	0.356	$3.50\cdot10^{-4}$	$3.89\cdot10^{-4}$
14	HIWP3-047	2.71	14.8	0.36	4.53	24.86	0.336	370	2.04	2.03	1.40	2.08	12.1	0.41	0.337	$5.20\cdot10^{-4}$	$9.04\cdot10^{-4}$
15	HIWP3-072	25.0	10.0	0.15	3.50	26.16	0.104	361	1.44	2.31	1.86	1.24	7.7	0.07	1.134	$1.08\cdot10^{-3}$	$1.96\cdot10^{-3}$
16	HIWP3-073	50.0	10.0	0.15	3.50	26.16	0.104	361	1.44	2.31	1.86	1.24	7.7	0.07	1.323	$2.40\cdot10^{-3}$	$2.66\cdot10^{-3}$
17	HIWP3-074	25.0	15.0	0.37	4.56	24.81	0.350	371	2.06	2.02	1.39	1.24	7.1	0.26	1.491	$4.52\cdot10^{-3}$	$1.15\cdot10^{-2}$
18	HIWP3-075	50.0	15.0	0.37	4.56	24.81	0.350	371	2.06	2.02	1.39	1.24	7.1	0.26	1.510	$1.43\cdot10^{-2}$	$1.18\cdot10^{-2}$
19	HIWP3-076	25.0	20.0	0.59	5.52	23.47	0.826	381	2.61	1.75	1.19	1.24	6.8	0.64	1.661	$2.66\cdot10^{-2}$	$3.31\cdot10^{-2}$
20	HIWP3-077	25.0	20.0	0.59	5.52	23.47	0.826	381	2.61	1.75	1.19	1.24	6.8	0.64	1.661	$2.58\cdot10^{-2}$	$3.31\cdot10^{-2}$
21	HIWP3-078	50.0	20.0	0.59	5.52	23.47	0.826	381	2.61	1.75	1.19	1.24	6.8	0.64	1.661	$6.27\cdot10^{-2}$	$3.31\cdot10^{-2}$
22	HIWP3-079	25.0	25.0	0.80	6.36	22.13	1.24	393	2.32	1.52	1.07	1.24	4.70	0.72	1.783	$6.26\cdot10^{-2}$	$4.23\cdot10^{-2}$
23	HIWP3-081	50.0	20.0	0.59	5.52	23.47	0.826	381	2.61	1.75	1.19	1.24	6.76	0.64	1.661	$7.90\cdot10^{-2}$	$3.31\cdot10^{-2}$
24	HIWP3-082	50.0	25.0	0.80	6.36	22.13	1.24	393	2.32	1.52	1.07	1.24	4.70	0.72	1.783	$1.83\cdot10^{-1}$	$4.23\cdot10^{-2}$
25	WP3/Test22	22.0	12.3	0.25	4.00	25.55	0.197	365	1.73	2.18	2.69	1.32	13.3	1.11	1.196	$5.00\cdot10^{-2}$	$2.83\cdot10^{-2}$

Note: grey colour - inhomogeneous mixture experiments

4 Conclusions

Two original localised mixture deflagration models developed at Ulster are presented for use as contemporary tools for hydrogen safety engineering. The models have been validated against experimental data on hydrogen-air mixture deflagrations available in the literature including experiments with stratified gas distributions carried out by KIT (Germany) and HSE (UK). The closed vessel model predictions were found to be within a +13%/-3% of the experimental data while the vented deflagration model predictions were found to be within +186%/-77% of the measurements.

The first model is based on the laws of thermodynamics and calculates the overpressure from localised mixture deflagrations in closed structures. The upper limit of hydrogen inventory that could be released and then burned in a closed structure with a strength of 10 kPa is derived using the model. This upper safety limit is equivalent to 7.9% of the closed space being filled with 4% hydrogen. Hydrogen inventories above this value would be expected to cause damage to stuctures having a strength of 10 kPa while hydrogen inventories below this value may or may not cause damage (if there were locally high overpressures due to flame acceleration through a congested region damage could still result).

The model and the correlation for vented deflagrations of localised gas mixtures, including non-homogeneous mixtures has been presented for the first time. The model allows vent sizing of low-strength equipment and buildings to mitigate adverse consequences of localised deflagrations for people and property. The theory demonstrates that only a small fraction of a non-uniform mixture with the highest burning velocity defines the maximum overpressure of a vented localised deflagration. The developed best fit correlation reproduces the experimental data with the best accuracy when the burning velocity range is taken as 95-100% of the maximum burning velocity. The conservative correlation is recommended for safety design of hydrogen systems and infrastructure. The coefficients for both the best fit correlation (A=0.018, B=0.92) and the conservative correlation (A=0.080, B=0.92) are derived.

The significance of this study is in the provision of contemporary tools for safety engineers needed for hazard and risk analysis, and the design of deflagration mitigation systems using venting technique for localised mixtures, which were not available before. The results of this joint work of international team underpin the inherently safer deployment of infrastructure with indoor use of hydrogen.

5 Acknowledgements

The research was supported by Fuel Cell and Hydrogen Joint Undertaking through the project "HyIndoor" ("Pre-normative research on safe indoor use of fuel cells and hydrogen systems"), grant agreement No. 278534, www.hyindoor.eu, and NET-Tools ("Novel Education and Training Tools based on digital applications related to Hydrogen and Fuel Cell Technology"), grant agreement No. 736648, https://www.h2fc-net.eu/.

6 References

1. Tamanini, F., "Partial-volume deflagrations – characteristics of explosions in layered fuel/air mixtures", Proc. 3rd Int. Seminar on Fire and Explosion Hazards (ISFEH3), Lake Windermere, England, pp.103-117 (2000).
2. Buckland, I. Explosions of gas layers in a room size chamber, Institution of Chemical Engineers Symposium Series, 58 (1980).
3. Whitehouse, D.R., Greig, D.R., Koroll, G.W., "Combustion of stratified hydrogen-air mixtures in the 10.7 m3 combustion test facility cylinder", Nuclear Engineering and Design 166:453-462 (1996).
4. Molkov, V.V., "Unified correlations for vent sizing of enclosures at atmospheric and elevated pressures", J. Loss Prev. Process, 14:567-574 (2001).
5. Stamps, D., Cooper, E. III, Egbert, R., Heerdink, S. and Stringer, V., "Pressure rise generated by the expansion of a local gas volume in a closed vessel", Proc. R. Soc. A (2009) 465, 3627–3646 (doi:10.1098/rspa.2009.0140).

6. Flamm, L., Mache, H. Die “Verbrennung eines explosiven Gasgemisches in geschlossenem Gefäß. Sitzungsberichte der Kaiserlichen Academie der Wissenschaften in Wien”, Klasse IIa 126:9–44 (1917).
7. Lewis, B., von Elbe, G., Combustion, flames and explosions of gases, p. 371, 2nd edn, New York, NY: Academic Press Inc. (1961).
8. Sibulkin, M., “Pressure rise generated by combustion of a gas pocket”, Combust. Flame, 38:329–334 (1980). (doi:10.1016/0010-2180(80)90063-2)
9. Babkin, V., Kononenko, Yu., Vykhristyuk, A. , Krakhtinova, T. , Krivulin, V. and Kudryavtsev, E., “Combustion of local gas volume in closed vessel”, Fizika Goreniya i Vzryva, 21:43–50 (1985).
10. Boyack K.W., Tieszen S.R., and Stamps D.W., “Internal pressure loads due to gaseous detonations”, Proc. R. Soc. Lond. A 443, 343–366 (1993). (doi:10.1098/rspa.1993.0150)
11. Yao C., “Explosion-venting of low-strength equipment and structures”, Int. J. Loss Prevention, 8(9) (1974).
12. Pasman, H.L., Groothuizen, Th.M., de Gooijer, H., “Design of pressure relief vents”, In: Loss Prevention and Safety Promotion in the Process Industries, Ed. by C.H. Bushman, pp.185-189, 1974.
13. Bradley, D., Mitcheson, A., “The venting of gaseous explosions in spherical vessels”, Combustion and Flame, 32:221-236 and 237-255 (1978).
14. Molkov, V.V., Nekrasov, V.P., “Dynamics of gaseous combustion in a vented constant volume vessel”, Combustion, Explosion and Shock Waves, 17(4):363-370 (1984).
15. Bauwens, C.R., Chaffee, J., Dorofeev, S.B., “Effect of ignition location, vent size and obstacles on vented explosion overpressure in propane-air mixtures”, Combust. Sci. Tech. 182 (11):1915-1932 (2010).
16. Bauwens, C.R., Chao, J., Dorofeev, S.B. , “Evaluation of a multi peak explosion vent sizing methodology”, Proc. 9th Int. Symposium on Hazards, Prevention and Mitigation of Industrial Explosions, Krakow, Poland, 22-27 July 2012.
17. Molkov, V., Dobashi, R., Suzuki, M., and Hirano, T., “Modeling of vented hydrogen-air deflagrations and correlations for vent sizing”, Journal of Loss Prevention in the Process Industries, 12:147-156 (1999).
18. Molkov, V., Grigorash, A., Eber, R., Tamanini, F., and Dobashi, R. “Vented gaseous deflagrations with inertial vent covers: state-of-the-art and progress”, Process Safety Progress, 23 (1):29-36 (2004).
19. Molkov, V., Bragin, M., “Hydrogen-air deflagrations: vent sizing correlation for low-strength equipment and buildings”, Int. Journal of Hydrogen Energy, 40(2):1256-1266 (2015).
20. Friedrich, A., Grune, J., Jordan, T., Kotchourko, A., et al. Experimental study of hydrogen-air deflagrations in flat layer, 2nd Int. Conference on Hydrogen Safety (ICHS2007), San-Sebastian, Spain, 11-13 September 2007.
21. Yanez, J., Kotchourko, A., Kuznetsov, M., Lelyakin, A., Jordan, T. Modeling of the flame acceleration in flat layer for hydrogen-air mixtures. 4th Int. Conference on Hydrogen Safety (ICHS2011), San Francisco, USA, 12-14 September, 2011.
22. Razus, D.M., Krause, U., Comparison of empirical and semi-empirical calculation methods for venting of gas explosions, Fire Safety Journal, 36:1-23 (2001).
23. Jallais S., Kudriakov S., An inter-comparison exercise on engineering models capabilities to simulate hydrogen vented explosions, Int. Conf. Hydrogen Safety, Brussels, Belgium, 9-11 September 2013.
24. Hooker, P., Hoyes, J., Hall, J., Willoughby, D. Experimental studies on vented deflagrations in a low strength enclosure, Int. J. Hydrogen Energy, 42(11):7565-7576 (2017).
25. Sinha, A., Rao, V., Wen, J. Evaluation of Engineering Models for Vented Lean Hydrogen Deflagrations, 26th Int. Colloquium on the Dynamics of Explosions and Reactive Systems (ICDERS), Boston, USA, 30 July – 4 August 2017.

26. Sustek, J., Janovsky, B. “Comparison of empirical and semi-empirical equations for vented gas explosion with experimental data”, Int. Journal of Loss Prevention in Process Industries, 26:1549-1557 (2013)
27. NFPA 68, Guide for Venting of Deflagrations. National Fire Protection Association, Quincy, MA, USA, 2013.
28. Kuznetsov, M., Friedrich, A., Stern, G., Kotchourko, N., Jallais, S., L'Hostis, B. Medium-scale experiments on vented hydrogen deflagration, J. Loss Prevention in the Process Industries, 36:416-428 (2015).
29. Kee, R., Rupley, F., Miller, J. CHEMKIN-II: A Fortran Chemical Kinetics Package for the Analysis of Gas-Phase Chemical Kinetics, Sandia National Laboratories Report, SAND89-8009, September 1989.
30. Morley, C., GASEQ - A chemical equilibrium program for Windows, http://www.gaseq.co.uk/ (accessed February 2015).
31. Baker, W., Cox, P., Westine, P., Kulesz, J., Strehlow, R. Explosion hazards and evaluation. Elsevier Scientific Publishing Company, 1983.
32. Mannan, S. “Lees' loss prevention in the process industries”, 3rd ed., V.1., Elsevier Butterworth-Heinemann, 2005.
33. Molkov V., Venting gaseous deflagrations, DSc Thesis, VNIIPO, Moscow, 1996 (in Russian).
34. Lamoureux, N, Djebaili-Chaumeix, N, Paillard, C.-E., “Flame velocity determination for H2-air-He- CO2 mixtures using the spherical bomb”, Experimental Thermal and Fluid Science 27:385-393 (2003).
35. Ross, M.C., Lean combustion characteristics of hydrogen-nitrous oxide-ammonia mixtures in air, Engineer’s thesis, California Institute of Technology (1997) (http://resolver.caltech.edu/CaltechETD:etd-01182008-143226)
36. Babkin, V.S., Private communication. Institute of Chemical Kinetics and Combustion, Siberian Branch, Russian Academy of Science, Novosibirsk, Russia (2003).
37. Molkov, V., Makarov, D., Puttock, J. “The nature and large eddy simulation of coherent deflagrations in a vented enclosure-atmosphere system”, Journal of Loss Prevention in the Process Industries, 19(2-3):121-129 (2006).
38. Molkov, V., Makarov, D., and Schneider, H. “LES modelling of an unconfined large-scale hydrogen-air deflagration”, Journal of Physics D: Applied Physics, 39(20): 4366-4376 (2006).
39. Makarov, D., Verbecke, F., Molkov, V., “Numerical analysis of hydrogen deflagration mitigation by venting through a duct” Journal of Loss Prevention in the Process Industries, 20(4-6): 433-438 (2007).
40. Makarov, D., Verbecke, F., Molkov, V. et al., “An inter-comparison exercise on CFD model capabilities to predict a hydrogen explosion in a simulated vehicle refuelling environment” Int. J. Hydrogen Energy, 34(6): 2800-2814 (2009).
41. Baraldi, D., Kotchourko, A., Lelyakin, A. et al., “An inter-comparison exercise on CFD model capabilities to simulate hydrogen deflagrations in a tunnel” Int. J. Hydrogen Energy, 34(18): 7862-7872 (2009).
42. Molkov, V., Verbecke, F., and Makarov, D. “LES of hydrogen-air deflagrations in a 78.5-m tunnel”, Combustion Science and Technology, 180(5):796-808 (2008).
43. Xiao, H., Makarov, D., Sun, J. and Molkov, V., “Experimental and numerical investigation of premixed flame propagation with distorted tulip shape in a closed duct”, Combustion and Flame, 159:1523-1538 (2012).
44. Keenan, J., Makarov, D., and Molkov, V. “Rayleigh-Taylor instability: Modelling and effect on coherent deflagrations”, Int. J. Hydrogen Energy, 39(35):20467-20473 (2014).
45. Karlovitz, B., Denniston, D.W.Jr., Wells, F.E., “Investigation of turbulent flames”, The Journal of Chemical Physics 19(5):541-547 (1951).

46. Molkov, V.V., Nekrasov, V.P., Baratov, A.N., Lesnyak, S.A., “Turbulent gas combustion in a vented vessel”, Combustion, Explosions and Shock Waves, 20:149-153 (1984).
47. Zimont, V.L., Lipatnikov, A.N., “A numerical model of premixed turbulent combustion of gases”, Chem. Phys. Reports 14(7): 993-1025 (1995).
48. Gostintsev, Yu.A., Istratov, A.G., Shulenin, Yu.V., “Self-similar propagation of a free turbulent flame in mixed gas mixtures. Combustion”, Explosion and Shock Waves 24(5):63-70 (1988).
49. Bradley, D., “Instabilities and flame speeds in large scale premixed gaseous explosions”, Phil.Trans. R.Soc. London A., 357:3567-3581 (1999).
50. Yakhot, V. Propagation Velocity of Premixed Turbulent Flames, Combust. Sci. Technol., 60(1-3): 191-214 (1988).